Deanship of Graduate Studies
Al-Quds University

An Advanced Approach to Reconstruct CT Images from limited-angle projections, reducing radiation dose and tube load.

Doaa Hosni Samarah Bani Odeh

M.Sc. Thesis

Jerusalem - Palestine

1445/2024

An advanced approach to reconstruct CT images from limited-angle projections, reducing radiation dose and tube load.

Prepared by
Doaa Hosni Samarah Bani Odeh

B.Sc.: Medical Imaging Science, AL-Najah National University, Palestine

Supervisor: Dr. Mohammad Hjouj

A Thesis Submitted in Partial Fulfillment of The Requirement for the Degree of Master of Medical Imaging Technology/Graduated Studies, Al-Quds University.

1445-2024

Al-Quds University
Deanship of Graduate Studies
Faculty of Health profession
Functional imaging course

Thesis Approval

An advanced approach to reconstruct CT images from limited-angle projections, reducing radiation dose and tube load.

Prepared by: Doaa Hosni Samarah BaniOdeh
Registration number: 22010037
Supervisor: Dr. Mohammad Hjouj

Master Thesis submitted and accepted, Date: 12/12/2023

The names and signatures of the examining committee members are as follows:

1- Head of the committee: Dr. Mohammad Hjouj Signature:

2- Internal Examiner: Dr. Sawsan Abu Sharkh Signature:

3- External Examiner: Dr. Ali Abu Arrah Signature:

Jerusalem-Palestine
1445 - 2024

Dedication

This research is dedicated to

Family, Instructors, and Colleagues.

Declaration

I certify that this thesis submitted for the degree of master's is the result of my research, except where otherwise acknowledged, and that the thesis has not been submitted for a higher degree to any other university or institution.

Signed:

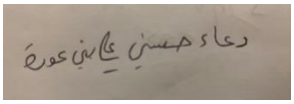

Doaa Hosni Samarah Bani Odeh

Date:12 / 12 / 2023

ACKNOWLEDGEMENT

I acknowledge everybody supports me in my thesis, Big thanks to my supervisor: Dr Mohammad Hjouj for his confidence. I am extremely grateful to radiologists, medical imaging technologists, and statisticians, for their help in image and data assessment.

I’m grateful to my father and mother for their encouragement and support to Study at the Graduate School.

Doaa Hosni Samarah Bani Odeh

Contents

list of abbreviations

Abbreviation	Definition
ADMIRE	Advanced Modeled Iterative Reconstruction
AEC	Automatic Exposure Control
AIDR 3D	Adaptive Iterative Dose Reduction 3D
ALARA	As Low As Reasonably Achievable
ART	Algebraic Reconstruction Technique
ASIR	Adaptive Statistical Iterative Reconstruction
AWTV	Adaptive Weighted Total Variation Minimization
CNR	Contrast Noise to Ratio
CT	Computed Tomography
DAS	Data Acquisition System
EM	Electromagnetic
FBP	Filter Back Projection
FIRST	Forward Projected Model-based Iterative Reconstruction Solution
FSIM	Feature Similarity Indexing Method
HU	Hounsfield Unit
IMR	Iterative Model Reconstruction
IR	Iterative Reconstruction
IRIS	Iterative Reconstruction in Image Space
KV	Kilovoltage
MBIR	Model-based Iterative Reconstruction
MSE	Mean Squared Error
NRMSD	Root-Mean-Square Deviation
PSNR	Peak signal to Noise Ratio
RwATV	Reweighted Anisotropic Total Variation Minimization
SAFIRE	Sonogram-Affirmed Iterative Reconstruction
SAH	Specialized Arab Hospital
SART	Simultaneous Algebraic Reconstruction Technique
SNR	Signal to Noise Ratio
SSIM	Structural Similarity Index Measure
TV-LR	Total Variation Low Rank
TVM	Total Variation Minimization
USA	United States America
WLS	Weighted Least Squares
Z	Atomic Numbers

List Of Figures

List Of Tables

An advanced approach to reconstruct CT images from limited-angle projections, reducing radiation dose and tube load

Abstract

Concerns regarding ionizing radiation doses to individuals and patients have arisen as a result of the remarkable advancements in computed tomography (CT) technology and applications over the last ten years, so Computed tomography (CT) scanners and CT exams have increased continuously. Researchers aim to minimize ionizing radiation dose via introducing new CT protocols and providing diagnostic CT images with lower radiation doses to patient. Nevertheless, these investigations have challenges: reducing the radiation dose results in decreased image quality, which might occasionally be non-diagnostic. In This study, the researcher aims to investigate the possibility of forming a CT brain image from a limited number of projections at a projection angle of less than 180 degrees While maintaining image quality based on the ALARA principle and decreasing radiation dose. then determine if the images match the quality criteria of Brain CT. This effort spanned from January 2023 to September 2023.

The process of reconstructing CT scan images from limited angle projections is critical and requires strict adherence to the ALARA principle. This principle is designed to minimize radiation exposure while maintaining image quality. Our study utilized filter back-projection (FBP) and algebraic iterative reconstruction (IR) algorithms to reconstruct brain CT images from 500 projection lines with a 100 x 100 and 200 x 200 matrix size. In addition to researching the effect of the reconstruction angle on image quality, two degrees were taken at an angle of 90 and 45 degrees. The images were evaluated for image quality criteria by 10 expert medical imaging technicians and 2 radiologists and specific evaluations were given. Then, a simple descriptive statistical analysis was conducted, including calculating percentages for expert medical imaging technicians and radiologists evaluations and p-values.

By combining the results of a MATLAB 2021 functions with the insights of a radiologist, we can produce high-quality images that decrease radiation dose and tube load. Our findings reveal that the algebraic method is superior to the filter back-projection in preserving image quality when utilizing limited-angle projections. In addition to the Statistical t-test (P<.001), which confirms the existence of statistical differences between the two algorithms. With a percentage of 41%, or a moderate scale, the IR algorithm matches quality requirements better. Conversely, the FBP exhibits a proportion of < 25%, signifying a weak scale.

Based on the percentages of evaluation, we can confirm that the size of the Matrix 200 x 200 is superior to the size of the Matrix 100 x 100, as it formed a percentage of 36.25%, which is equivalent to a moderate scale. In addition, the reconstruction angle of 90 provides better quality and its percentage was 41.75%, equivalent to a moderate scale. So the IR algorithm at 90 degree with 500 projection only provides images that match the quality criteria for brain CT. while FBP fails to provide any meaningful insights when working with angles of 45 and 90 degrees.

Keywords: CT scan, Iterations Reconstruction (IR), Filter Back Projection (FBP), radiation Dose, ALARA, Image Quality.

Chapter 1

Introduction

This chapter outlines the problem statement (section 1.1) , justification of research (section 1.2), and discusses the Study Objective of research (section 1.3), Furthermore, (section 1.4) the limitations of the study .

1.1Problem statement

Computed Tomography (CT) represents the largest contribution of the total radiation dose from medical radiation . It represents about one-half of total radiation according to the United States America (USA) due to the exponential increase in the demand for CT scan procedures. it's important to make a great effort in an attempt to reduce radiation dose , to match ALARA (as low as reasonably achievable) for reducing patient dose to have to try to decrease the risk of the possibility of deterministic effects or stochastic effect while maintaining image quality .

1.2justification

Based on the principle of ALARA that concluded all medical diagnostic procedures ought to be as low as reasonably achievable . it's anchored on the radiation assurance recommendation of international expert committees to create the core of radiation protection (Yu *et al.*, 2009) .

Computed Tomography (CT) has two competing aspects . on the one hand , has effective advanced applications and tools to define and detect disorders such as pulmonary embolism , appendicitis , renal stone et cetera. On the other hand , has much more potent to deliver radiation that causes cancer or different risks . Radiation exposed risks can be categorized into two patterns: Deterministic effect from cell death , and stochastic effect which constitutes the main risk from CT dose exposed. (Kalra *et al*., 2004)

The amount of absorbed dose determines the chance of a stochastic effect. In actuality, the type of examination, the patient's age, and the radiation exposure quantity all affect the

outcome of radiation exposure. For instance, repeated head CT scans or lenses exposed to threshold radiation doses may result in the production of cataracts (5 H). Thus, leukemia (P) can result from exposure to certain tests; the list of possibilities is endless. Different tests and techniques involving modest dosages of CT images must be produced.(Hobbs *et al.*, 2018)

1.3 Study Objective

This study's main objective is to offer a technique that produces respectable image quality at lower doses. In particular, the three following hypotheses will be investigated in this work:

1. Limited angle CT reconstruction decreases radiation dose.

2. Limited-angle CT reconstruction with Filter back projection FBP dose sacrifices image quality more than Algebraic iterative reconstruction (IR).

3. The effect of Matrix size and the angle of reconstruction on image quality for limited angle image.

1.4 Limitations of the Study

- Lack of relevant local literature, research, and resources examining the connection between CT dose and the impact of limited angle.

- The difficulty of using MATLAB 2021 on a non-advanced HP PC, which hinders or cancels many steps.

- Difficulty obtaining a copy of the MATLAB 2021 program.

Chapter 2

Literature Review and Theoretical Background

This chapter talks about computed tomography and dose reduction strategies especially iterative reconstruction (IR) that must be explained then talks about image quality. It also includes previous studies according to the history from the past to the present. Through the chronology, it was found that some studies have confirmed providing an algorithm to eliminate artifacts caused by limited projection, but it is not similar to our study methodology .

2.1Background of the Study

Radiation is a form of energy that is characterized by its ability to penetrate and interact with different parts. Ionizing radiation and non-ionizing radiation are the two types of radiation. The two other categories of ionizing radiation are electromagnetic (EM) radiation and particle radiation. High-intensity electromagnetic radiation, including X-rays and gamma rays, can quickly and painlessly penetrate biological tissue. This denotes that it falls under the ionizing radiation category and is typically applied to diagnose and treat patients instead of surgery in minimally invasive treatments (Almasri and Inayyem, 2021).

The introduction of Computed Tomography (CT) scan as a key diagnostic modality in 1972 marked the second revolution in the area of diagnostic imaging (Tepper, 2008). From spiral scanning in 1980 to the introduction of multidetector-row technology in 1990, the CT application was then developed (Kalender *et al.*, 1990). With significant advancements in quality, resolution, accuracy, and speed, the applications of CT have continued to grow rapidly (Crawford and Kina, 1990). This made it possible to quickly and safely replace surgical diagnostic procedures with the CT scan, which has an isotropic spatial resolution of 0.3–0.4 mm and a fast scanning speed (Yu *et al.*, 2009).

Despite the fact that CT offers valuable information for diagnosis and patient care, the CT modality can result in malignancy when risks and benefits are combined(National Research Council, 2006). It is clear that reducing CT radiation dose remains one of the most critical

and valuable projects in this field because it contributes the most to overall medical radiation exposure.

Radiation exposure is a sufficiently major factor to affect the accuracy of CT imaging and diagnosis. It is essential to understand the correlation between the image's quality and CT dose reduction to know the quantity of dose can be reduced without sacrificing quality. Reducing the amount of radiation used must be done under circumstances that ensure that image quality is not compromised. The aim of dose reduction can be briefly stated from two approaches. The first one

sets the correct goal for image quality and aims for a specific diagnostic task. From a second perspective, one might consider enhancing some aspects of image quality, such as minimizing noise, reducing radiation dose, or raising CNR and SNR. (Lee and Chhem, 2010) .

To increase dose efficiency, a great deal of effort has been put into developing generic dose reduction procedures (King, McCarter and Davis, 1982). Some of these efforts are dependent on the optimization of the CT system, which involves several different system elements, including the collimator, beam-shaping filter, and detector. others may be determined by the scan range, Automatic exposure control, dual-energy CT, and Some logarithms, with Iterative reconstruction (IR) being the most significant of these. (Lee and Chhem, 2010) (Yu *et al.*, 2009)

2.2Computed Tomography and Radon

2.2.1 Principle of Computed Tomography

The word tomography has two roots, tomo, meaning to section, cut, or layer. The other one is the graph, representing a scan. At first glance, Tomography is a phrase that may seem novel at first, yet its roots can be found in the early 1920s. Then, in the 1930s, a tomographic technique was created to obtain transverse cross-section. Transverse axial tomography was the name of the method used to provide specifics for human body diagnostics. (Eliason, 2022)

Computed Tomography (CT) produces radiography that’s able to discriminate between tissues of similar density by scanning sections of the body with a narrow X-ray beam that

rotates around the body. Then use a sophisticated computer algorithm to turn the data into axial cross-sectional slices of the human body. In comparison with conventional radiography, the CT modality can offer radiography at a specific level with the capability of differentiating between two components with modest density changes. (Romans, 2011)

Each CT slice represents a specific plane at z thickness referred to as the z-axis, see Fig (2.1) with a specific level. The thickness can be determined by the scanner to limit the x-ray beam by a small shutter device called a collimator, so the beam passes just through this volume, hence. diminishing scatter radiation. (Romans, 2011)

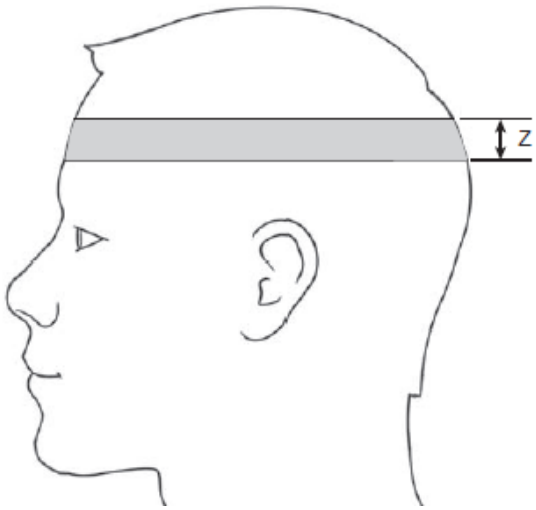

Figure 2.1: Z axis as the thickness of the cross-sectional slice (Romans, 2011).

Pixels are two-dimensional squares that are used in CT radiography. The CT image is made up of several pixels. A voxel is created when the Z axis is taken into account, whereas a matrix is created when dealing with rows and columns of pixels. 512 is the most common matrix size. see Fig (2.2).

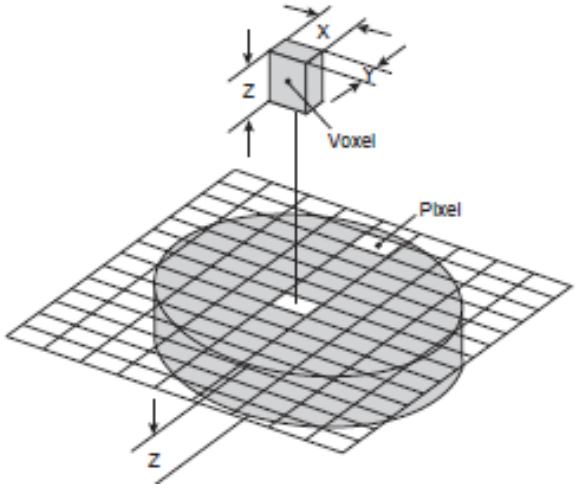

Figure 2.2: The element of the data that form the CT slice (Romans, 2011)**.**

2.2.2 Component of Computed Tomography

Different parts of computed tomography (CT) are primarily responsible for producing clear images of cross-sectional anatomy. The most crucial of these parts are the X-ray tube and detector (Zeng, 2010). The information obtained during a CT scan is X-ray transmission through human tissue that has had some interaction. To acquire an image from the patient, components of the imaging device housed in the gantry cooperate. (Eliason, 2022) .

2.2.2.1Gantry

The section that surrounds the patient in a ring shape is called the gantry. It contains a number of parts, including the DAS, an X-ray tube, a detector, a high-voltage generator, a collimator, and a slip ring. Gantries come in a variety of aperture sizes, commonly ranging from 70 to 90 cm in diameter. The CT gantry can be tilted between a range of +/- 15 and +/- 30 degrees. An additional laser light on the gantry is utilized to locate the patient's isocenter position. The light can be controlled via a control panel located at the side of the opening gantry . The gantry tilt and table movement can both be controlled by technologists using the control panel. A microphone is consequently installed in the gantry to enable communication between patient and radiation technicians. See Fig (2.3) (Romans, 2011).

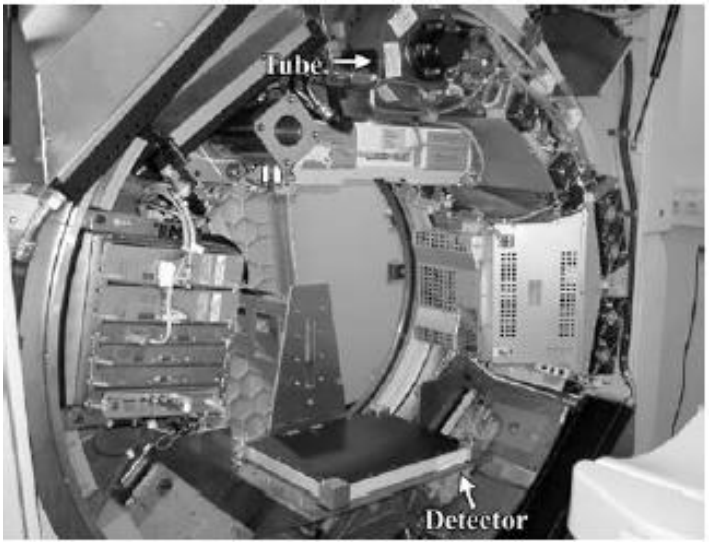

Figure 2.3: The components of the CT gantry (Eliason, 2022).

2.2.2.2 Slip ring

Because using recoiling system cables to rotate the gantry frame limited gantry rotation, early CT scanners were designed to scan in a step-and-shoot mode. However, modern systems use slip rings, which are electromechanical devices with brush-like apertures that provide continuous electrical power and electronic communication. This enables the gantry frame's continuous movement to produce helical scan modes. (Romans, 2011) See Fig (2.4).

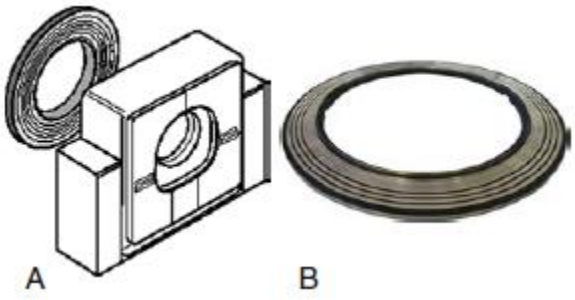

Figure 2.4: The types of slip ring (A) disk design (B) The pancake type. (Eliason, 2022)

2.2.2.3Generator

Currently, CT employs high generators near the gantry because they are compact enough. Previously, CT used extremely stable three-phase generators, but these are now obsolete because they are stand-alone close to the gantry and require cables.

The X-ray tube received high voltage according to the generators' activity. The range of exposure techniques is determined by the amount of power generated in kilowatts which is the capacity of power, so the generator's ability to produce high KV typically 120 to 140 KV allows for a reduction in patient dose by enhancing penetration and also helps to lessen the heat load on the X-ray tube by producing low mA settings, extending the tube's lifespan. (Romans, 2011)

2.2.2.4Cooling system

Due to the temperature-sensitive components, gantry cooling is a crucial factor. Multiple types of cooling systems exist. such as filters, blowers, or equipment that generates heat exchange from oil to air. (Romans, 2011)

2.2.2.5X-ray Source

The beam of X-ray photons required to make CT radiography is frequently created by X-ray tubes. A higher-intensity X-ray beam is produced by tungsten material when used as an anode because of the proportional relationship between intensity and atomic number of the target material.

Usually, The focal spot sizes of X-ray tubes typically range between 0.5 and 1.0 mm. The smaller one is utilized to create superior resolution (a sharper image), which lowers penumbra. (Eliason, 2022)

2.2.2.6Filtration

Because the polychromatic X-ray beams produced by CT tubes must be shaped, compensating filters are used to filter the long-wavelength X-ray energy that would otherwise increase the patient dose. and therefore reduce beam hardening-related artifacts to further enhance image quality (Romans, 2011) see Fig (2.5).

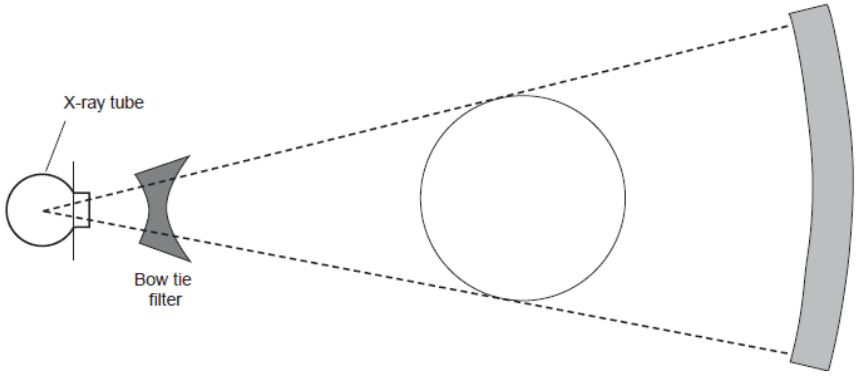

Figure 2.5: The Bow tie filter as a common type of filter. (Romans, 2011)

2.2.2.7Collimation

Collimators are used as a device to confine the X-ray beam to a certain area. They have a small shutter. By doing this, scatter radiation is decreased, which leads to better image quality and a lower radiation dose for the patient. (Romans, 2011)

By narrowing and broadening the X-ray beam, the collimator, which was placed close to the X-ray source, limited the X-ray and restricted it, allowing the technologist to select the thickness of the slice and how the dose is spread across it. It is frequently referred to as pre-patient collimations since it occurs before the patient receives the X-ray. (Romans, 2011)

pre-detector collimators are used in some CT systems to shape the beam after it. passes through the patient and prevents scatter radiation from reaching the detector. these collimators are situated between the patient and the detector. (Romans, 2011)

2.2.2.8Detector

As the X-ray penetrates through the patient and interacts, it is somewhat attenuated. Information on the amount that each anatomical structure attenuated the beam should be gathered. Thus, utilizing the detector in CT as a tool for data collection. Detector arrays are a phrase used to describe the group of detectors in a CT system. (Romans, 2011) See Fig (2.6)

The size of the beam, which in turn determines the number of element detectors that expose radiation, can be determined through the use of a restricted FOV. There are numerous

configurations for detectors, including single configuration and multi-slice configuration. Irrespective of the detector setup type. The detector is constructed of several materials. (Romans, 2011)

The optimal characteristics and properties of a detector are as follows: 1) The efficiency of the detector to capture transmitted photons and change them to electronic signal should be high which is based on several factors. These are stopping power, scintillator efficiency, charge collection efficiency , geometric efficiency and scatter rejection. 2) no or low afterglow. 3) elevation scatter depressed. 4) and stability system . (Romans, 2011)

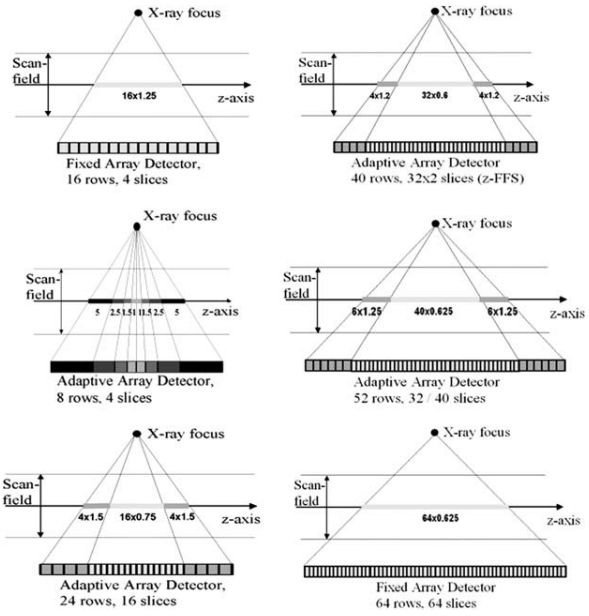

Figure 2.6: The Configuration of array CT detectors and types. (Kohl, 2005)

2.2.3 Beam Attenuation

In CT radiography, different gray scales are used to illustrate the various ways that X-ray beams interact with objects. an X-ray beam consists of a bundle of energy (photons). this energy may be passed through an object or absorbed others photons are redirected by scattered. the photons that pass through the object are represented as black pixels (low attenuation), While photons that are absorbed are shown as white pixels (high attenuation), and implicitly the intermediated attenuation as a gray shade. The quantity of photons that interact with an object relies on several factor : photon energy itself, thickness, density, and

the atomic number of the object, so the number of photons increases by increasing the atomic number, thickness, and density. (Romans, 2011)

The quantity of the X-ray beam that is scattered or absorbed per unit thickness of the object is represented by the linear attenuation coefficient, which is denoted as μ. As the atomic number and density increase, the attenuation coefficient often does too. As the energy of the photons increases, it lowers. Consequently, the variations among tissues are to blame for X-ray contrast . (Zeng, 2010)

The Hounsfield Unit (HU) is a unit used in CT to assess the attenuation of various tissues. It is also known as the density value or CT number. The amount that a structure attenuates an X-ray beam can be measured by HU. Based on the fact that water has a HU value of zero, this unit is derived. All objects that attenuate less than water have a corresponding negative number, such as air, which has a value of -1000 HU. Positive HU values are seen in substances that attenuate more than water, such as bone with 1000 HU. Keep in mind that the linear attenuation coefficient and HU value are correlated. (Romans, 2011)

Every X-ray transmission line simply has a relationship to a certain attenuation value reconstruction after passing through a 2D patient slice in a given direction. According to Beer's law, X-rays attenuate . Wherefor is the Attenuation coefficient (μ) dependent on material and x-ray energy see equation 1 . (Eliason, 2022)

$$\text{CT number} = \mu - \mu_w / \mu_w \times 1000 \qquad (1)$$

where μw is the attenuation coefficient of water. in computed tomography, intensity measurements are made for many line-integral paths confined to a plane, Image reconstruction from a line of X-ray means projection was based on the theory of the Austrian mathematician Radon from 1917. Who based his theory on the possibility of reconstructing the image of a 2D or 3D object from a large number of its projections from different directions. (Romans, 2011)

2.3 Dose Reduction Strategies

The rate of radiation that the patient receives from the CT scanner is estimated at 1–14 mSv depending on the type of exam. Based on statistics on CT usage from 1991 to 1996, one study hypothesized that up to 0.4% of all malignancies that are currently diagnosed in the United States may be caused by radiation from CT exams. It was found that 1.5–2% of malignancies may someday be brought on by the ionizing radiation used in CT when organ-specific cancer risk was adjusted for present levels of CT usage. This eventually resulted in an aggressive effort to minimize CT doses and optimize image quality. Concurrently, new technologies and algorithms such as iterative reconstruction (IR) were in development and eventually made commercially available for all current CT. (McCollough *et al.*, 2009)

2.3.1 CT system

The improvement of the CT system's detector, collimator, and shape filter's dose efficiency is largely due to its development.

1) Detector

The detector is the fundamental CT component that controls the dose performance of the CT system. Its geometrical efficiency and detection efficiency give an impression of how well the detector performs its function of converting incident X-ray to signal. (Yu *et al.*, 2009)

The primary obstacles to dosage reduction are image noise from electronic noise and quantum noise. Image quality is lowered as the amount of photons is decreased. Therefore, all electrical parts of the X-ray detecting system should be upgraded and refined when dealing with low dosage inspection.(Yu *et al.*, 2009)

2) Collimators

For constrained X-ray beams, there are two different collimators available. First, a pre-patient collimator is placed between the patient and the x-ray source to define the x-ray beam coverage and prevent undesirable radiation dose to the patient. the second type of collimator, the post-patient collimator, which is placed between the patient and the detector to limit scatter radiation.to reduce scatter radiation which preserves and improves image quality, but sacrifices dose so it’s necessary to carefully assess between image quality and dose. (Jaffray and Siewerdsen, 2000)

3) X-ray beam shaping

The filter plays a key role in attenuating the beam spectrum, which makes it possible for the X-ray radiation dose to be hard enough to penetrate the patient while still producing adequate contrast information. Since the amount of attenuation in the center is typically greater than the peripherally, filters like the bowtie that increase attenuation at the peripherals also enable minimizing radiation dose, particularly the dose to the skin. (Toth *et al.*, 2005)

2.3.2Scan range

The scan range should be kept small as possible as and large as necessary to avoid direct radiation exposure for any parts of the body that are not necessarily included for diagnosis because the scan range has a direct relation to the total radiation dose delivered to the patient. (Yu *et al.*, 2009)

1) Automatic Exposure control (AEC)

AEC is used to modulate the tube current automatically to be suitable with differences in attenuation due to patient anatomy shape and size. the tube modulates based on a function of projection angle or longitudinal location along the patient or both.

To achieve optimal radiation level for any patient with adequate image quality for example: less tube current for small patient then less dose. therefore obtain desired image quality and for a large patient to obtain adequate image the radiation dose must be increased.(Wilting *et al.*, 2001)

2.3.3Optimal tube current

Numerous clinical studies have demonstrated that the amount of dose reduction or improved image quality occurs while utilizing lower tube potential. For instance, Funama and Nak have demonstrated that when the patient weighs 80 kg, it is feasible to lower the KV setting from 120 to 90 KV in an abdomen CT operation without affecting the image quality of the low contrast.(Funama *et al.*, 2005) (Nakayama *et al.*, 2005)

An iodine contrast agent is required for CT exams. The hyper- or hypovascular diseases are enhanced by the iodine enhancement at lower tube potentials. (Yu *et al.*, 2009)

2.4 Limited-Angle CT Reconstruction

The limited angle CT reconstruction acquisition process is well approximated by the linear imaging model . Unlike traditional routine CT, which uses x-ray measurement to provide across-sectional images from a full viewing angle (0-180). An alternative to this is to reconstruct a limited angle from a limited radon projection or when a portion of the view is obscured, such as [0, max], "max" 180. reconstruction in this case, is highly ill-possed see Fig (2.7). (Anirudh *et al.*, 2018)

Although limited angles result in artifact-laden reconstruction, they have advantages. By restricting the scanner's movement and limiting the scan to just the region of interest, together with reducing patient dose, scan times can be reduced. (Anirudh *et al.*, 2018)

It's interesting in the 1980s, researchers investigated two algorithms for traditional CT reconstruction, referred to as the simultaneous algebraic reconstruction technique (SART) and the algebraic reconstruction technique (ART), respectively. (SART)(Kak, A.C., no date). Noise and artifacts appeared in the reconstruction image during the application of the preceding two techniques at a limited angle.dealing with limited-angle reconstruction recently. The iterative reconstruction algorithm is thought to be the best available because it offers greater advantages than the traditional filter back projection (FBP) algorithm, which provides a quick and accurate analytical solution to reconstruct the image, but delivered images with inadequate resolution, especially when dealing with low dose levels. (Yu and Zeng, 2015)

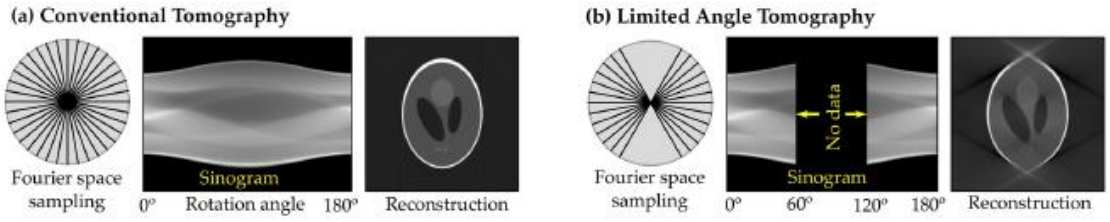

Figure 2.7: Comparison of limited angle and conventional computed tomography**.** (Barutcu *et al.*, 2021)

Filter back projection (FBP) is an analytic algorithm that is based on a single reconstruction . Through the use of a high pass filter and back projection, it is raised from

CT slices that are reconstructed from sonograms (Beister, Kolditz and Kalender, 2012) As the name indicates, it consists of two primary steps: the first is executing the back projection operation, but since it's a non-negative function, it is insufficient for reconstruction. In order to remove the blurring, the second stage involves applying a negative wings (filter) (Zeng, 2010) The rapid reconstruction time of FBP is an advantage, but the main drawback is that the raw data is placed into a "black box" so that the limited model and prior information can be employed.

Iterative reconstruction is a computer tomographic algorithmic method that utilizes geometric and statistical models to variably weight the image data . Because iterative statistical reconstruction methods use several repetitions in which the current solution converges in relation to the best solution, they safely eliminated radiation exposure by 27% to 76% without significantly sacrificing image quality. thus, Iterative statistical reconstruction methods achieve a safely lower radiation dose. (Seibert, 2014)

All iterative reconstruction algorithms contain three main steps which are repeated iteratively, as visualized in Fig (2.8). First, a forward projection of the volumetric object estimate that is used to create artificial raw data which, in the next step, are compared to the real measured raw data to count a correction term. In the final step, the correction term is back-projected onto the volumetric object estimate. The iteration process reconstruction is usually initiated by using prior information or an empty image estimate, such as a volume of a similar object or a standard FBP reconstruction. In general, the better result is when the prior images match the final images. The iteration must have an end, so it’s finished when either a steady number of iterations is reached, when a predefined quality criterion in the image estimate is fulfilled, or when the update for the current image estimate is considered small sufficient (Beister, Kolditz and Kalender, 2012) .

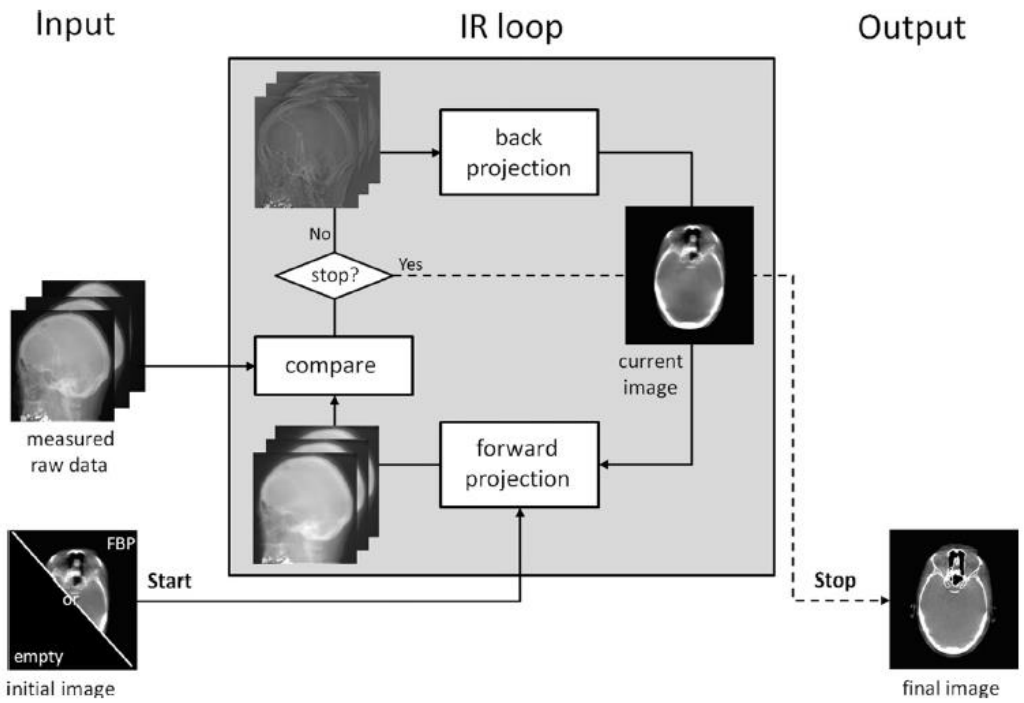

Figure 2.8: graphical view of the iterative reconstruction process . (Beister, Kolditz and Kalender, 2012)

From the 1970s , the first scanners are already used IR algorithms starting with ART, but due to lack of computational power, the IR algorithm took until the 2009s to become commercially available instead of conventional FBP. One has to keep in mind that FBP is still in use today , But the need to produce an optimal radiological image quality with low doses of radiation based on the principle of ALARA , prompted researchers to develop the IR algorithms . These developments are classified into three approaches :

1) image domain based .
2) sinogram based .
3) fully iterative algorithm .

In the 2009s, the iterative reconstruction in image space IRIS received FDA clearance as the first IR algorithm. This was a simple way that similar to FBP which means only a single backward projection was applied to create a cross-sectional image from raw data. After that, during two years three advanced IRs were classified under the hybrid IR algorithm:

ASIR (Adaptive Statistical Iterative Reconstruction), iDose4, and SAFIRE (sonogram-Affirmed Iterative Reconstruction). This type works as FBP and IRIS single backward projection step applied. However, hybrid IR is considered a more advanced IR Method since after iteratively filter is applied to raw data to reduce artifacts, and after backward will apply the filter at the image to reduce image noise. Also during this period other most advanced IR so far received FDA clearance, but it was classified as the first fully IR method, the so-called VEO. In fully IR the raw data are backward projected into the cross-sectional image space then are forward projected to create artificial raw data. After that, the raw data is compared with true raw data to update the cross-sectional. The operation of backward and forward projection is stopped when the difference between artificial and true data is minimized. Another hybrid IR algorithm most recently in 2016s, is another model-based IR called FIRST (forward projected model-based iterative reconstruction solution). Other model–based and hybrid IR algorithms were introduced with different vendors see Table (2.1). Numerous studies have proven that the IR is superior to the FBP in improving image quality and reducing radiation dose see Fig (2.9). Other studies confirmed that the dose is reduced further with model-based IR compared to hybrid IR and FBP. (Willemink and Noël, 2019)

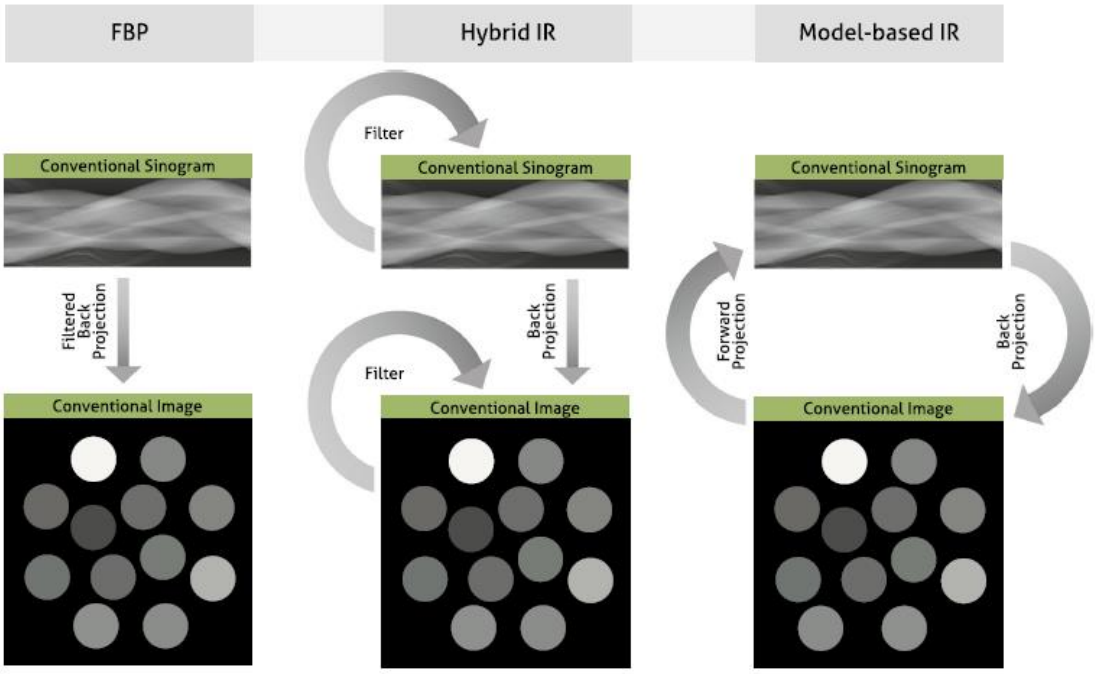

Figure 2.9: Schematic view of the Filtered back projection (FBP), hybrid iterative reconstruction (IR) and model-based IR. (Willemink and Noël, 2019)

Table 2.1: Different types of iterative reconstruction algorithms with the name vendors.

Vendor name	Algorithm name	Type of Algorithm	Artifact reduction	Noise reduction
GE Healthcare.	- ASIR. - Veo (MBIR). - ASIR-V.	- Hybrid . - Model-based . - Hybrid .	- Average . - Strong . - Average.	- Strong . - Very strong. - Strong .
Philips Healthcare .	- iDose^4 . - IMR.	- Hybrid . - Model-based.	- Average . - Strong .	- Strong . - Very strong .
Siemens Healthineers .	- IRIS . - SAFIRE . - ADMIRE .	- Image domain. - Hybrid. - Model based.	- Minimal . - Average . - Strong .	- Average . - Strong . - Very strong .
Canon Healthcare .	- AIDR3D . - FIRST .	- Hybrid . - Model based .	- Average . - Strong .	- Strong . - Very Strong .

2.5 Previous Studies

To the best of our knowledge, there are no previous studies similar to the methodology based on this study, which aims to demonstrate the effectiveness of CT-limited-angle reconstruction in reducing radiation dose to the patient while maintaining acceptable diagnostic image quality. This chapter will present some studies related to limited-angle reconstruction by CT.

Rushil Anirudh et al 2018 , proposed a neural network to recover CT limiting angle (incomplete view sinogram) between 0-90 degree . by using at the beginning CTNet o embeds the limited angle sinogram into latent space with utilizes 1D CNN . 1D CNN promote use multiple filter with varying window size to capture different information via it . so been used 5 window size and 256 filter . this formulation back up varying number rows into inputs sinogram. therefore , used FBP to final reconstructed but noticed appear bluer at edge because the edge information missing at final reconstruct also used weighted least squares WLS as a model based IR . then to ensure getting smoothed image the CTNet training with mean squared error MSE to provide highest PSNR and structural similarity SSIM. on other hand used adversarial loss to generate more realistic looking reconstructions . as a result the analytic reconstruction such as FBP and WLS produces more accurate reconstruction compare to methods that direct predict the CT image . but based on PSNR and SSIM the WLS is significantly better than exiting approaches as a solution of sinogram completion . (Anirudh *et al.*, 2018)

Wei Yu et al 2015 , In order to reduce streak artifact and nearby edge artifact that FPB created in limited angle reconstruction, this study proposes an efficient image reconstruction optimization model based on ℓ0 gradient minimization to reconstruct limited angles between 0 to 90 and 0 to 120 degree, with interval 1mm via the projection views available 90 and 120, respectively. The developed algorithm for limited-angle tomography was tested using a digital NURBS-based cardiac-torso (NCAT) phantom with a matrix size of 256 × 256. Added Gaussian noise to the noise-free projection additionally. Comparing the suggested method to traditional IR methods including SART, which has more advantages than FBP, and TVM-based algorithms, which are frequently used for partial reconstruction projection data with the best parameter during TVM, would aid in

verifying the worth of the suggested approach first. Finally, after 1000 rounds, the PSNR and NRMSD measurements of the images were reconstructed using various techniques. As a result, it was discovered that the proposed algorithm performed better than both the TVM-based algorithm and the SART algorithm in terms of the PSNR and NRMSD measures because it provided good regularization function properties, which were defined as the ℓ0-norm of the image gradient (Yu and Zeng, 2015) . Another study used TV to preserve the edge well after denoising operation. Therefore, hongliang et al 2016, proposed an algorithm to suppress streak artifacts that occurred during limited-angle CT reconstruction Thus, the study proved that this approach can reduce the dose while reducing the edge and streak artifact and also providing high image quality compared with ART-TV, and MLN-TV. Then the SNR was calculated, so the proposed method outperforms the ART-TV algorithm and ART-TV algorithm by 40%, with 29% gains in term SNR measure. furthermore, more than 58%, 49% reduction in terms of MAE measure (Qi *et al.*, 2016) .

Similarly, Zhanli et al.'s 2017 study sought to minimize streak artifact by applying "TV-FR" during Ct reconstruction for limited projection via using a Micro-CT on an anesthetized mouse, 291 projections were uniformly collected over a 197.88° range using a proposed method based on the TV performed under penalized weighted least-squares (PWLS-TV) also Only 120 views were then applied at head phantom by spanning on a circular orbit of 360°. FBP was employed throughout implementation as the starting point for the first iteration of the picture reconstruction process. To recover the fine features lost in the TV minimizing and restore the structure details that were lost in the TV minimization, the feature refinement (FR) is then applied for each PWLS-TV iteration. Thus, a comparison was made between FBP, PWLS-TV, and PWLS-TV-FR. Because the RMSE value of PWLS-TV-FR is the lowest and the PSNR value of PWLS-TV-FR is the highest, which indicates and verifies the validity of the PWLS-TV-FR algorithm for limited angle CT reconstruction, it is obvious that PWLS-TV-FR achieves better performance than the other two algorithms for reducing streak artifact of the limited angle CT reconstruction(Hu *et al.*, 2017) . Moran XU et al. 2021, on the other hand, used FBP for dictionary limited angle projection, gradient l0-norm to get high quality images with clear images with little noise, and split Bregman to optimize the objection function, leading to

the term " ℓ0 DL" being used. Thus, Use numerical models and preclinical mice testing to evaluate the effectiveness of the new approach to FBP , TV, and TV with Low Rank (TV-LR). All reconstruction tests were carried out on the PC Mat Lap 2018 using the RMSE, SSIM, and FSIM calculators. Consequently, the RMSE in ℓ0 DL is the smallest compared to comparisons, although TV-LR method only slightly outperforms TV method. The SSIM and FSIM enhance in the proposed technique by enhancing several parameters that influence the power of DL, however the proposed method requires a significant amount of time because the model includes the terms gradient minimization and dictionary learning. (Xu *et al.*, 2021).

Furthermore, study of Mohammad Hjouj et al 2022, proposed a new algorithm for reconstruction an image in a plane limited number of radon projection. hypothesized that there is a linear relationship to which density is subjected to the production of new image, and based on this hypothesis it allow to map a uniformly distributed view angles over 180° to some range of view angles that are available for the original image which allow the transformed image is reconstructed from the uniformly distributed angles that correspond to a limited number of projections. ('DMIP22-K3006-Reconstruction-From-Limited-Angle-Projections-Based-on-Transformation-1', no date)

Jingyu Guo et al. 2016 the study aimed to present a new approach based on generating an optimized initial image followed by total variation (TV) depending on IR considering the feature of image symmetry to remove artifacts nearby edges from limited projection images. In addition to the proposed algorithm, the counters symmetry and mirroring filling technique was used. In this study, the limited angle image produced from fan beam limited angle CT and the X-ray source is located on Y-axis and X-axis with counterclockwise limited angle rotation by 150 – 120 degrees to collect projection data. The approach followed was verified by researching the qualitative and quantitative criteria during the comparison of the reconstructed image using the proposed algorithm, reconstructed from POCS-TV with initial zero image and reconstructed one from POCS-TV with initial FBP. Where the value of SNR was the highest possible, and the value of MSE was the lowest possible compared to POCS-TV with zero image and FBP image. Thus, the method was

applied to phantom and real CT scans, indicating that the proposed method effectively removes the artifacts nearby the edge. (Guo *et al.*, 2016) .

Moreover, Changcheng Gong et al 2020, compare the ARTV as a new method with TVM , ATV , AWTV and RwATV methods during conduct three group experiments on Forbild head phantom with different RMSE , PSNR , SSIM . it's has been figured out that ARTV methods provide image closer to reference image and as the scanning angular range increase , the reconstructed image quality is gradually get better . (Gong and Zeng, 2020)

2.6 Image Quality

Because of the complexity of CT image acquisition and display, image quality in CT can be difficult to preserve and maintain. To improve image quality, one should consider increasing density resolution, decreasing scan times, and improving spatial resolution . (Eliason, 2022)

Three factors primarily impact image quality in medical imaging: contrast, noise, and spatial resolution. In general, some of the key performance measures that may be used to assess the quality of a CT image include low contrast resolution, high spatial resolution, accuracy of CT number, artifact, and noise. The protocols used for the operation , such as KVP , mAss , slice thickness , helical pitch, matrix size , scan speed and reconstruction algorithm parameters also have an impact on these aspects.(Eliason, 2022)

2.6.1 Spatial Resolution

The CT scanner's spatial resolution refers to its capacity to distinguish between two closely spaced tiny objects. Line-pair test patterns are frequently used to evaluate limiting resolution. To resolve a line-pair test pattern, the space must be individually visible on the image. See Fig (2.10) (Eliason, 2022) .

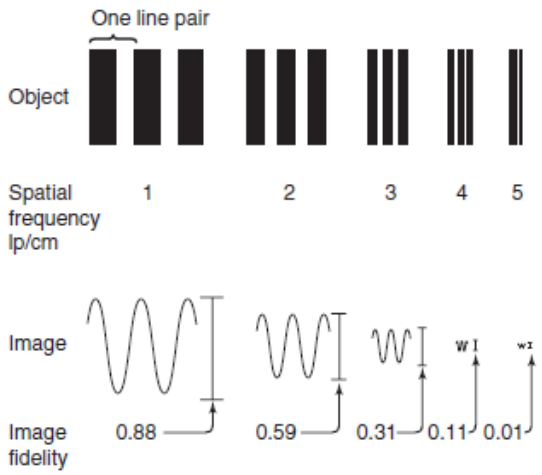

Figure 2.10: The test line pair of a bar pattern (object). (Eliason, 2022)

2.7.1 Factor That Affect Spatial Resolution

Numerous factors affect the spatial resolution. The most popular factor is manufacture factors included the x-ray focal spot size and shape , sampling frequency , detector cell size and scanner geometry . Manufacturers of CT could change these factors.

The spatial resolution is significantly impacted by two mathematical operations used in the reconstruction algorithm: back projection and convolution. for instance, blurring results if the projection profiles are back-projection outwards corrected. Consequently, a ramp filter is used before back-projection in order to sharpen and optimize the picture, as seen in Fig (2.11). For anatomically specific applications, other algorithms, such as kernel algorithms or convolution, have been developed to modify the appearance of image structures, such as bone kernels, to provide a significantly sharper image (better spatial resolution).(Eliason, 2022)

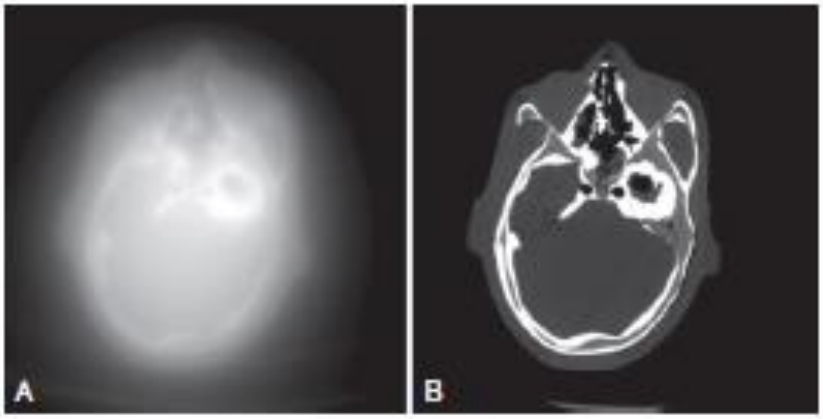

Figure 2.11: Impact of convolution process by head phantom . A) reconstruction with Back-projection . B) reconstruction with Filter Back- Projection . (Eliason, 2022)

The spatial resolution is additionally affected by the reconstruction field of view (FOV). To facilitate the visualization of little objects, the pixel size must be suitably small. The following equation relates the pixel size to FOV:

Pixel size = FOV/ Matrix size (2)

Based on the previous equation , 512 x 512 matrix sizes are often employed in conventional CT, so the theoretical size of one pixel is 0.625 mm , 0.31 mm for 1024 × 1024 Matrix size and 0.156 mm for 2048 × 2048 see Fig (2.12) . thus , a large matrix size preserved the spatial resolution and improved image quality despite an increase in image noise when compared to a 512 matrix size (Hata *et al.*, 2018) .

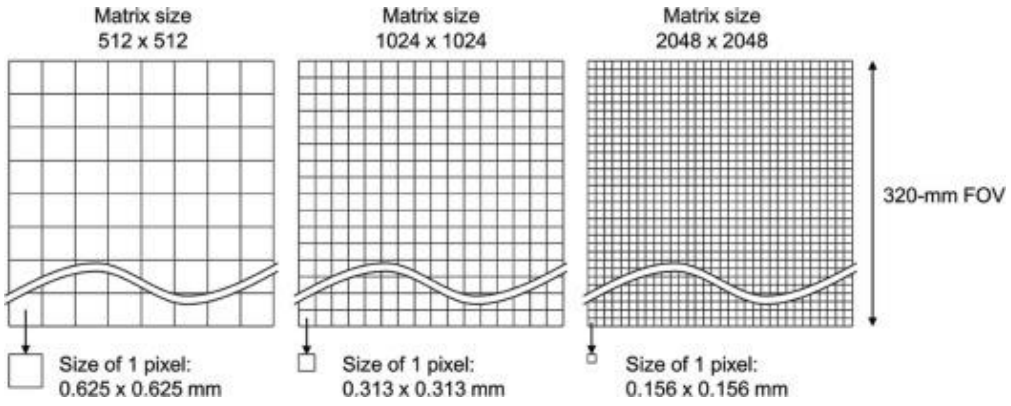

Figure 2.12: The relationship between the size of 1 pixel and matrix size .

2.6.2 Contrast Resolution

The most significant advantage of CT versus conventional radiography. it's capacity to identify things with low contrast and somewhat differing densities from the background. This is referred to as system sensitivity.

The contrast allows a CT system to distinguish between two objects with very identical densities to understand low contrast resolution see Fig (2.13) which contained three tissues of different atomic numbers (Z) and densities. due to CT can detect density differences from 0.25% to 0.5% , so CT can image tissues that vary slightly in density and atomic number (Z) such as fat and muscle are too close and appear as soft tissue shadow .

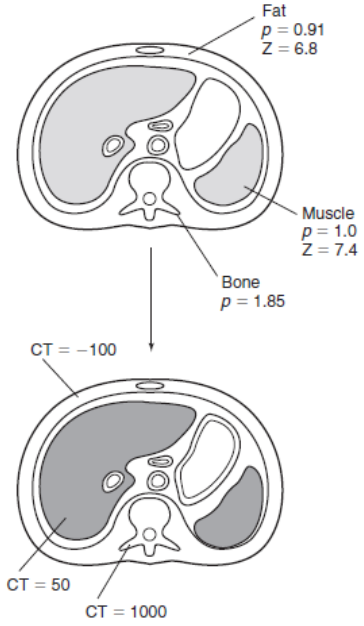

Figure 2.13: Densities and anatomic number (z) for three type of tissue : Fat , Bone and Muscle.

2.8.1 Factor Affecting Low Contrast Details (LCD)

The performance of CT imaging system by CT system parameters , mAss , KVP , beam collimation , pitch and slice thickness . Adjusting these parameters will improve image quality, reduce noise, and boost SNR. (Alsleem and Davidson, 2013) . see Fig (2.14)

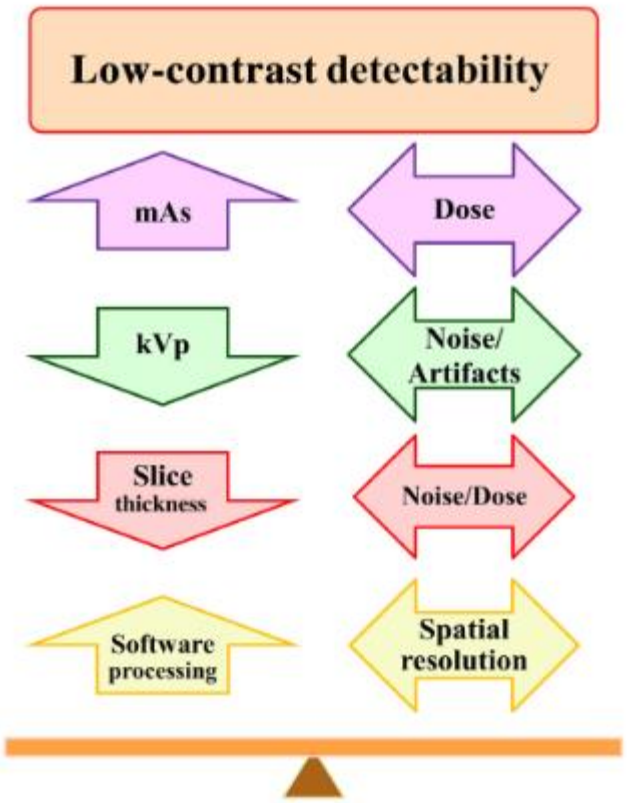

Figure 2.14 : Factors affecting low contrast detail (LCD) .(Alsleem and Davidson, 2013)

2.6.3 Noise

The noise in the image is caused by three different sources. The most important factor in determining the amount of observed x-ray photons is quantum noise, which is controlled by scanning technique variables such helical pitch, slice thickness, and scan speed.

The second source of noise is the inherent physical limitations of the system included electrical noise also the third noise influencing factor is the reconstruction parameter.

2.7 Quality Criteria for Brain CT

Calzao et al.(2000) Define five parameters for the quality of the image without contrast, which were later updated by the European Guidelines on CT image quality standards and served as a standards and benchmark for brain CT scans.These include the visual reproduction of the mesencephalon, the basal ganglia, the ventricular system, the border between white and grey matter, the cerebrospinal fluid space over the brain, and the visual

reproduction of the cerebrospinal fluid space around the mesencephalon.(Calzado, Rodríguez and Muñoz, 2000) . Fig (2.15) describes brain CT criteria during 5 points.

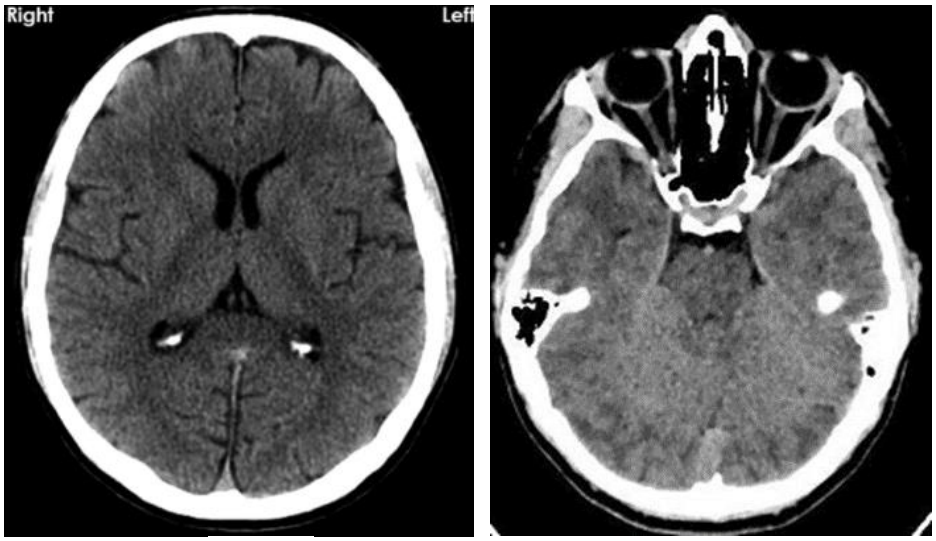

(a) (b)

Figure 2.15 : Brain CT criteria , a) sharp reproduction of the border between white and grey matter also sharp CSP , ventricles and basal ganglia. b) cerebrospinal fluid (CSF) around mesencephalon will be visualized.

Chapter 3

Material and Data Acquisition

This chapter provides an experimental framework of the study, from data collection to reconstructed CT Brain radiography by MATLAB 2021 and Quality criteria standards check. Then, compare the new reconstructed images with the parent images. The main focus was to assess the effects of limited angle reconstruction on CT dose while providing acceptable image quality based on the ALARA principle. The required data were collected from the Specialized Arab Hospital (SAH). This chapter describes the methodology adopted by this research to achieve the aims stated in section 1.3 of Chapter1 .

3.1 Setting

Brain CT standard procedure image from Medical Imaging Technologists at Specialized Arab Hospital (SAH) was used in the suggested investigation following a specified procedure as described in Table (3.1) . This study sought to determine the impact of limited angle reconstruction on CT dosage without significantly compromising image quality. The work concentrated on limiting angle reconstructing CT brain images using FBP and IR algebraic methods in MATLAB utilizing HP CORE i5 PCs Results were compared between two different limited-angle CT reconstruction methods at various angles . Reconstruction was done at 45 and 90 angles using both reconstruction methods : FBP and IR algebraic via 500 line of projection with 100 × 100 matrix size and 200 × 200 matrix size.

Table 3.1: The hospital protocol for Brain CT procedure.

Protocol	hospital helical protocol
kVp	120
mAs	380
Thickness	2.5
Increment	10
Filter	Brain standard
Center	40
Width	80
Acquisition type	Helical
Rotation time	.75

3.2 Study Duration

This research was conducted from 1/3/ 2023 to 1/9/2023 where the data collection was carried out from 1/3/2023 to 15/4/2020.

3.3 Study Design

This research is an experimental study was chosen to fulfill the aim of the study. Data was obtained from Imaging Department at Arab Specialized Hospital by taking Brain CT DICOM radiography with hospital protocol , reconstructed by IDose . among 3 brain CT radiography with normal case .

3.4 Study Population

All adult patients between the ages of 25 and 35 who have been requested to undergo brain CT using the routine protocol are included in the study population.

3.5 Inclusion and Exclusion Criteria

With the exception of patients who were pregnant, claustrophobic, or who declined to sign a patient permission form, all adult patients with normal situations were requested to do a brain CT scan .

3.6 Study Instruments

CT Philips ingenuity 128 slice, uses the fourth-generation IDose reconstruction algorithm**.** algebraic functions in MATLAB 2021 were utilized on an HP CORE i5 PC to construct new CT images and plots in diagnostic quality. Data was imported from Philips CT scanners in the form of CT DICOM images onto the researchers' personal computer. The MATLAB software was subsequently employed to form a 100x100 matrix size and 200 x 200 from the original image Fig (3.1). This matrix was then applied to create restricted reconstruction images through the application of two distinct reconstruction algorithms: Filter Back-Projection (FBP) and algebraic iterative reconstruction (IR) algorithms.

different function algorithm described in Table (3.2) . Other computer software’s has been used; radiant DICOM viewer.

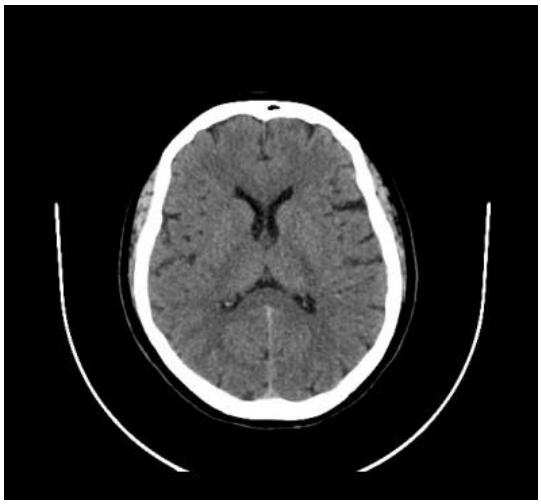

Figure 3.1: The original CT Brain radiography from CT Philips ingenuity 128 slice.

Table 3.2: Types of functions used in the study.

Protocol	First Function	Second Function	Third Function
Type of algorithm.	New original radiography	Filter Back Projection	Iterative Reconstruction
Matrix Size.	100 × 100 200 × 200	100 × 100 200 × 200	100 × 100 200 × 200
Degree of reconstruction	360 degree	45 / 90 degree	45 / 90 degree

3.7 Ethical approval

- In order to get permission and authorization to conduct the study, the study proposal was submitted to the Faculty of Graduate Studies review board at Al-Quds University. The approval was obtained on January 3, 2023.
- The study participant who shared in the study accepted sharing his medical information.

3.8 Quality Criteria for Brain CT

Ten expert medical imaging technologists took part in the effort to assess if the final images satisfy the reference study's quality criteria. The scale employed here by the researchers was 1 = weak, 2 = moderate, 3 = acceptable, and 4 = excellent. Then, they calculated the percentage of examinations for which the criteria were fulfilled from all medical imaging technologists' assessment. Here, the researchers compared two images, one with a brain IR algorithm, and the other with FPB algorithm.

Also , two radiologists participated to determine if the resulted images are diagnostic (1: not diagnostic, 2: diagnostic). After that, the researchers calculated the percentage of examinations for which the criteria were fulfilled.

3.9 Statistical Test

To compare the data and algorithms, simplistic descriptive statistical methods such as means and percentages were employed. The Paired Samples t-Test done between an iterative reconstruction and filter back projection to ensure that the IR provides the diagnostic appearance and that the images coincide the quality criteria for brain CT.

Chapter 4

Results and Discussion

The results in this study were divided into four groups (100 ×100 matrix size with 45 degree, 100 ×100 matrix size with 90 degree, 200 ×200 matrix size with 45 degree and 200× 200 matrix size with 90 degree) based on the parameter used: matrix size 100 × 100 or 200 × 200 and the angle of reconstruction (45 degree or 90 degree) and only 500 line of projection utilized. In each experiment, two different reconstruction method were used : a) Iterative reconstruction (IR) and b) filter back projection (FBP) . After that, all images were evaluated by ten expert technologist and two radiologist. Furthermore the hypothesis findings are shown, so this chapter outlines the results of the study and discussing them.

4.1 Results for Diagnostic Appearance

First, using functional (3,4,5,6) on MATLAB program 2021, the researchers derived new 100 × 100 and 200 × 200 matrix sizes from the original Brain CT image (Fig. 4.1), which was suitable for diagnosis.

```
New =zeros(M,M);                                    (3)
for i=1:M                                           (4)
for j=1:M                                           (5)
 New(i,j)  = P2(i,j); %image                        (6)
```

,Where M = 100 or 200 , i = x-axis , j = y-axis and P2= new image .

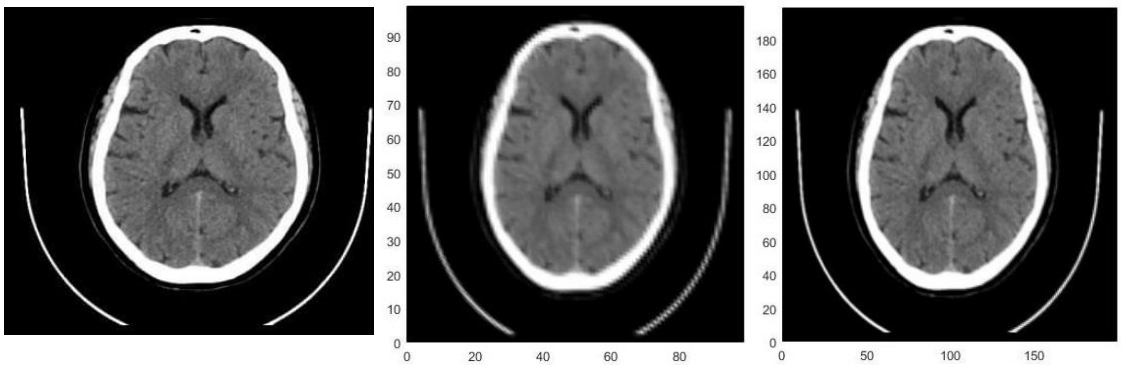

(a) **(b)** **(c)**

Figure 4.1: Computed tomography image of the brain , (a) The original CT brain

radiography from CT Philips ingenuity 128 slice. (B) new CT brain radiography with 100 × 100 matrix size . (C)) new CT brain radiography with 200 × 200 matrix size .

Figure 4.1.b was subjected to two experiments. In the first experiment, the image was reconstructed at an angle of 45 degree using 500 lines of projection based on the mathematical functional of MATLAB(7,8,9,10,11) which represents the filter back projection algorithm , and the mathematical functional (12,13,14,15) which represents the iterative reconstruction algorithm .These images were unacceptable in terms of diagnosis, as shown. In Fig (4.2), it is worth noting that the two algorithms failed to produce an image of acceptable quality. Also, as was the case in the second experiment, the same mathematical equations were used to produce images consisting of 500 lines, but at an angle of 90 degree , as shown in Fig (4.3).

```
Phi =0:1:45; or 90                                                    (7)
   [R0,xp0] = radon(flipud(New),Phi);% to know length(xp              (8)
   figure (2)
   plot( xp0,R0(:,1))                                                 (9)
   %now we well use iradon
   I0 = iradon(R0,Phi);                                              (10)
    I00 = imresize(I0, [M  M]);                                      (11)
    figure (3)
    colormap(gray);

PHIDEG =0:1:45;%0:1:80 ;  or 90                                       (12)
PHI = PHIDEG*pi/180;                                                  (13)
%PHI =linspace(0,pi/2,46);                                           (14)
numL= 1*floor(sqrt(4)*M);% number of lines per angle                  (15)
```

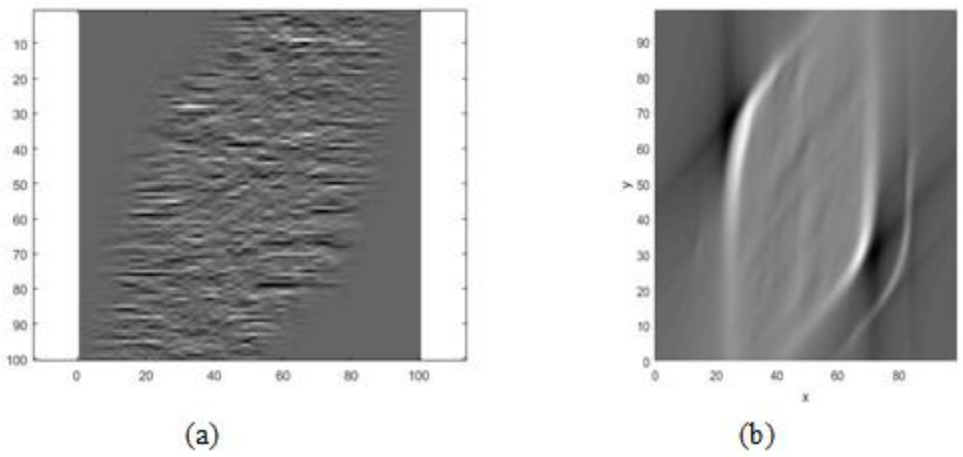

Figure 4.2: Brain CT radiography with 100 × 100 matrix size (a) 100 × 100 matrix size with IR algorithm for reconstruction of new original CT radiography at 45 degree (b) 100 × 100 matrix size with FBP algorithm for reconstruction of new original CT radiography at 45 degree.

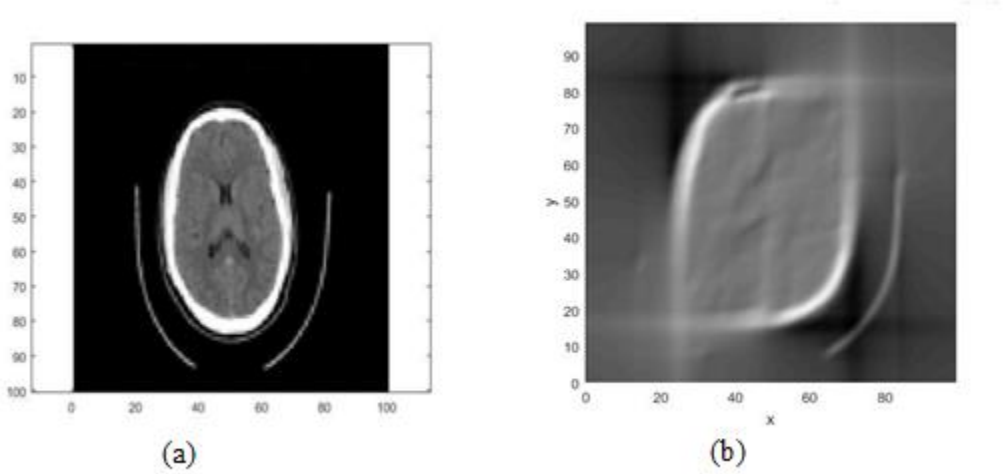

Figure 4.3 : Brain CT radiography with 100 × 100 matrix size (a) 100 × 100 matrix size with IR algorithm for reconstruction of new original CT radiography at 90 degree (b) 100 × 100 matrix size with FBP algorithm for reconstruction of new original CT radiography at 90 degree.

On the other hand, the same experiment was done using the same mathematical equations mentioned previously, which depend on two mathematical algorithms (IR and FBP), but using matrix size 200 × 200 with the same number of projections during two angle of

reconstruction 90 and 45 degree (figure 4.4 and figure 4.5) . The result for diagnostic appearance which was determined by the two radiologists is described in table (4.1). Where value 1 means not diagnostic and value 2 means diagnostic .

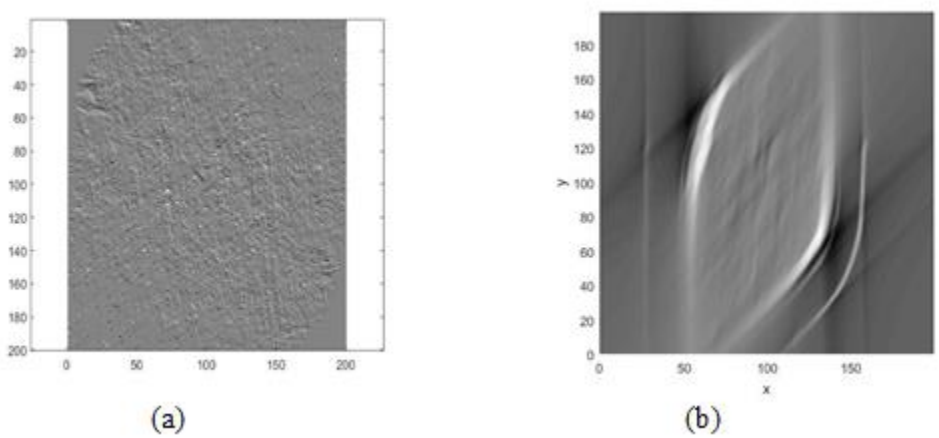

Figure 4.4: Brain CT radiography with 200 × 200 matrix size (a) 200 × 200 matrix size with IR algorithm for reconstruction of new original CT radiography at 45 degree (b) 200 × 200 matrix size with FBP algorithm for reconstruction of new original CT radiography at 45 degree.

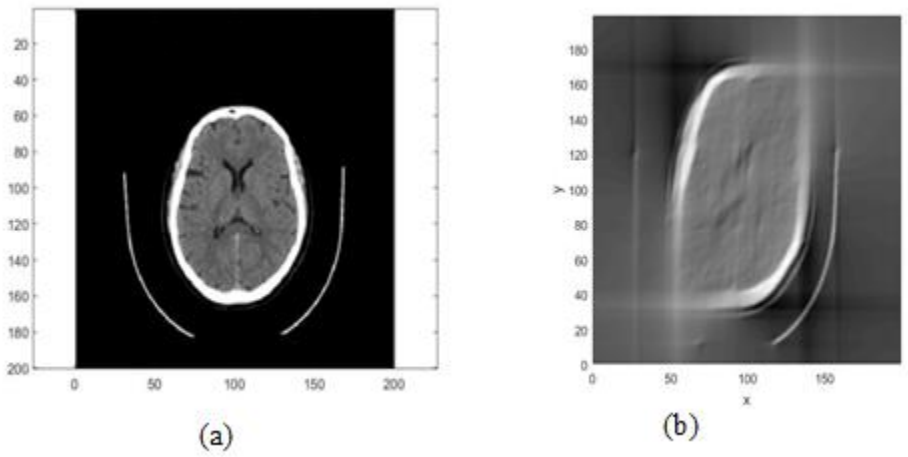

Figure 4.5: brain CT radiography with 200 × 200 matrix size (a) 200 × 200 matrix size with IR algorithm for reconstruction of new original CT radiography at 90 degree (b) 200 × 200 matrix size with FBP algorithm for reconstruction of new original CT radiography at 90 degree.

Table 4.1: Results from two radiologists for the diagnostic appearance after applying the MATLAB function for two algorithm, here, 1 means not diagnostic, 2 means diagnostic.

Case no	Radiologist 1		Radiologist 2	
	IR algorithm	FBP algorithm	IR algorithm	FBP algorithm
Case 1				
Fig 1.1	1	1	1	1
Fig 1.2	1	1	1	1
Fig 1.3	1	1	1	1
Fig 1.4	2	1	2	1
Case 2				
Fig 2.1	1	1	1	1
Fig 2.2	1	1	1	1
Fig 2.3	1	1	1	1
Fig 2.4	2	1	2	1
Case 3				
Fig 3.1	1	1	1	1
Fig 3.2	1	1	1	1
Fig 3.3	1	1	1	1
Fig 3.4	2	1	2	1

All Fig in appendix A.

4.3 Results for Quality Criteria for Brain CT

In this study, ten expert medical imaging technologists participated to determine if the resulting image matches the quality criteria scale. Here, the researchers used the following scale (1: weak, 2: moderate, 3: accepted, 4: excellent). Table (4.2) shows the result for quality criteria, and as shown, the IR algorithm at 90 degree with 500 projection only provides images that match quality criteria for brain CT.

Table 4.2: Expert radiographers assessment results for limited angle projection for brain CT Criteria by two algorithm and different parameters including matrix size and angle of reconstruction, the second Column represents the frequency, the third column represents the percent of frequency, the four column represents the status of quality criteria based on scale and the five column represents the percentage of criteria status.

	Frequency	Percent	Status	Percentage
Fig 1.1.a	10	100	Week	0-24.9%
Fig 1.1.b	10	100	Week	0-24.9%
Fig 1.2.a	1	10.0	Week	0-24.9%

	8	80.0	moderate	25-49.5%
	1	10.0	Accepted	50-74.9%
Fig 1.2.b	10	100	Week	0-24.9%
Fig 1.3.a	10	100	Week	0-24.9%
Fig 1.3.b	10	100	Week	0-24.9%
Fig 1.4.a	2	20.0	moderate	25-49.5%
	8	80.0	accepted	50-74.9%
Fig 1.4.b	10	100	Week	0-24.9%
Fig 2.1.a	10	100	Week	0-24.9%
Fig 2.1.b	10	100	Week	0-24.9%
Fig 2.2.a	3	30.0	week	0-24.9%
	6	60.0	moderate	25-49.5%
	1	10.0	Accepted	50-74.9%
Fig 2.2.b	10	100	Week	0-24.9%
Fig 2.3.a	10	100	Week	0-24.9%
Fig 2.3.b	10	100	Week	0-24.9%
Fig 2.4.a	2	20.0	moderate	25-49.5%
	5	50.0	accepted	50-74.9%
	3	30.0	perfect	75-100%
Fig 2.4.b	10	100	Week	0-24.9%
Fig 3.1.a	10	100	Week	0-24.9%
Fig 3.1.b	10	100	Week	0-24.9%
Fig 3.2.a	10	100	moderate	25-49.5%
Fig 3.2.b	10	100	Week	0-24.9%
Fig 3.3.a	10	100	Week	0-24.9%
Fig 3.3.b	10	100	Week	0-24.9%
Fig 3.4.a	4	40.0	moderate	25-49.5%
	6	60.0	accepted	50-74.9%
Fig 3.4.b	10	100	Week	0-24.9%

All Fig at appendix A.

4.4 Statistical Test for Quality Criteria Brain CT

The scale that the researchers used: 1 = weak, 2 = moderate, 3 = acceptable, and 4 = excellent .Subsequently, they computed the percentage of examinations for which all of the medical imaging technicians' evaluations fulfilled the requirements. Thus, these criteria were expressed in the following percentages(0-24.9% , 25-49.5% , 50-74.9% , 75-100%) respectively. Here, the researchers compared two algorithm IR and FBP as algorithm for reconstruct of limited angle with different matrix size also different angle of reconstruction, As shown in (Fig 4.6 and Fig 4.7). The IR algorithm has a better match for quality criteria, determined by the reference study with a percentage of 41% , which correlates to a moderate scale. On the other hand, the FBP has a percentage of < 25%, which correlates to

a weak scale. In addition There are statistically significant differences, which means that there is no chance in the results of this research, where the Statistical t-test (P<.001) .

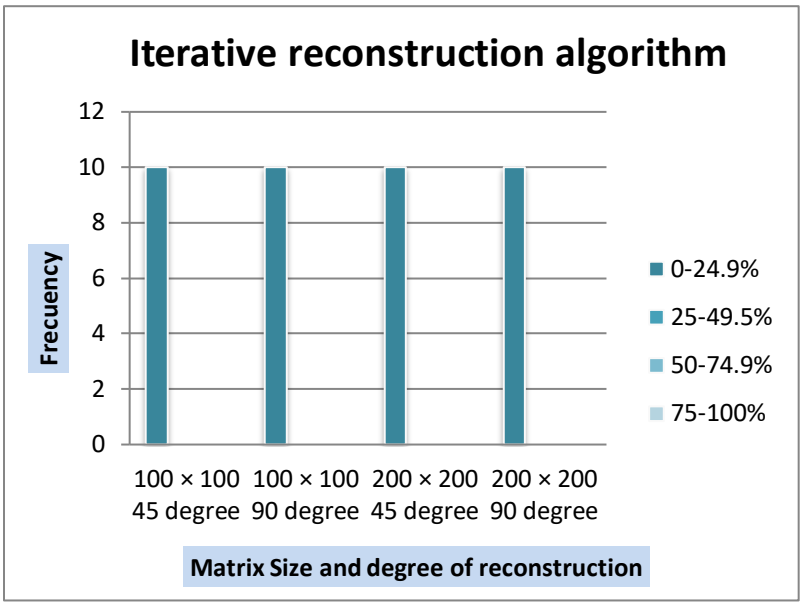

Figure 4.6: The percentage of quality criteria for iterative reconstruction algorithm resulting from the expert medical imaging technologists evaluation with changes in matrix size and angle of reconstruction .

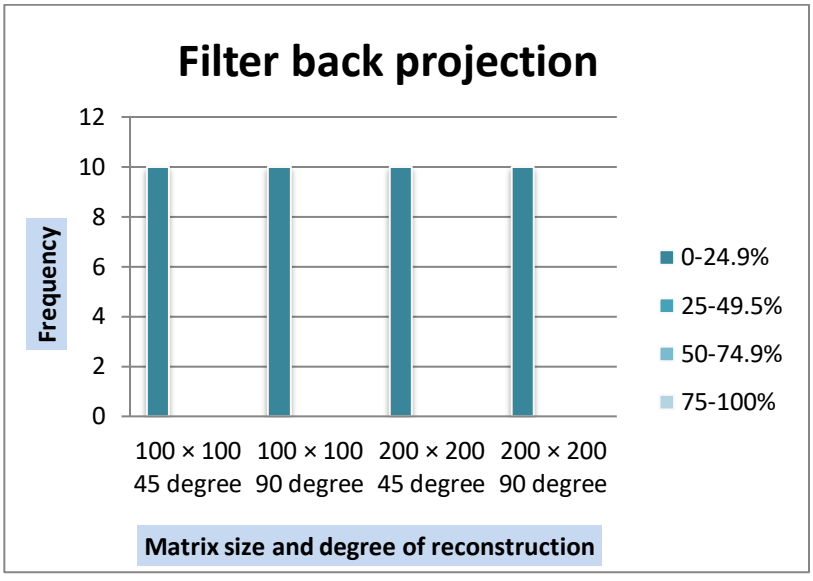

Figure 4.7: The percentage of quality criteria for filter back projection algorithm resulting from the expert medical imaging technologists evaluation with changes in matrix size and angle of reconstruction .

Figure 4.6 and Figure 4.7 shows the result for the average of all parameters that affected the image quality ,therefore, the study investigated the effect of changing the matrix size and image reconstruction angle, as Fig (4.8). It shows that the matrix size of 200 × 200 represents a percentage of 36.25% , which is equivalent to the moderate estimate, while 100 × 100 represents a percentage of 30.7% , as the matrix size of 200 × 200 is superior in providing better image quality .

Figure (4.9) also shows the percentages of the reconstruction angle, which shows a percentage of 41.75% with an moderate estimate for a 90 degree reconstruction angle while <25% for a 45 degree reconstruction angle. Which means that the 90 angle is superior in providing better image quality.

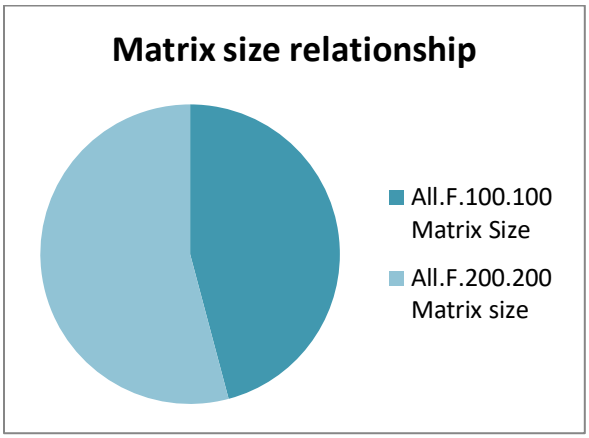

Figure 4.8 : The percentage relationship between 200 × 200 and 100 × 100 matrix size.

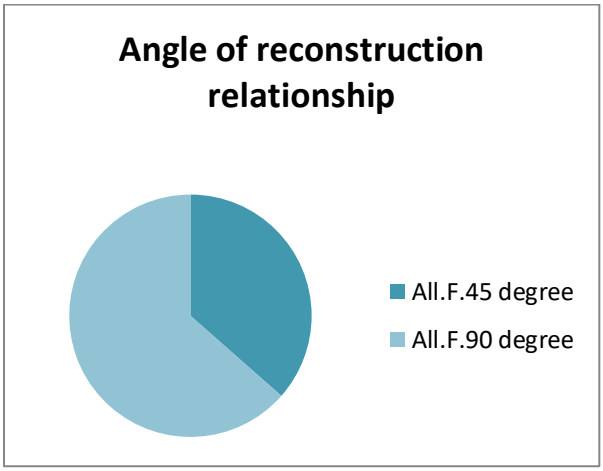

Figure 4.9 : The percentage relationship between 90° and 45° reconstruction angle.

5.5 Brief results for Diagnostic Appearance

In this study two radiologists participated to determine and decided if the resulted radiograph provided any diagnostic appearance , so table (4.3) concludes the summary of their assessment's findings for the limited angle reconstruction pictures.

Table 4.3: The final results for the radiologist tests with a diagnostic appearance for the limited angle reconstruction images of 500 projection only.

	Radiologist 1	Radiologist 2
200 200 matrix size 90 degree with IR algorithm	diagnosis	diagnosis

4.6 Discussion

Through a meticulous examination of quality standards by a proficient radiologist and expert medical imaging technologist also an in-depth analysis of MATLAB results, it has been determined that generating CT images using limited angle projections is a viable option. This innovative technique can effectively minimize patient radiation exposure and tube loading via reduce the x-ray projection that interact with patient organ and it can drastically reduce scan time by restricting the physical movement of the scanner , As a result of the proportional relationship between scan time and radiation dose , the radiation dose gradually decreases.

In the realm of reconstructing images from limited angle projections while preserving their quality, algebraic iterative reconstruction (IR) algorithm outperforms filter back-projection (FBP). FBP fails to provide any meaningful insights when working with angles of 45 and 90 degree . In contrast, the IR algebraic method significantly improves image quality, which was confirmed by Yu and Zeng's study in 2015. In addition to the Statistical t-test ($P<.001$), which confirms the existence of statistical differences between the two algorithms.

It's important to note that using a 100 x 100 pixel matrix size may not provide accurate diagnoses. The matrix size is a crucial factor in image quality, as demonstrated by Haney Alsleem's research. A larger matrix size preserves spatial resolution and enhances image quality, although there may be an increase in image noise compared to a 512 matrix size,

as noted in Hata et al.'s 2018 study. Therefore, based on figure (4.8), which shows the superiority of the Matrix 200 × 200 in providing better image quality.

Based on figure (4.9), an angle of 90 degree is considered the best angle compared to an angle of 45 degree in improving image quality. This depends on the fact that by increasing the angle of reconstruction, there will be an increase in the scan field of view .

4.7 Conclusion

This study marks a significant milestone in our country's efforts to generate brain CT images from limited angle projections and assess the quality criteria for algebraic IR and FBP methods. The findings indicate that producing diagnostic images from limited angle projections can be accomplished through the use of more sophisticated computers that can handle larger matrix sizes and more cases. The data gathered during this study is a valuable source for researchers who are striving to reduce radiation exposure to patients during CT scans while maintaining image quality and minimizing tube loading.

Limited angle projection of Brain CT reconstruction with only 500 projection provides a diagnostic appearance and a match quality criteria for brain CT, after applying a MATLAB functions we have a sharp match for quality criteria when use algebraic IR especially with matrix size 200 × 200 and 90 degree for angle of reconstruction .

4.8 Future perspective

This study indicated the possibility of producing a CT image while reducing the number of projections, which helps reduce the radiation dose to the patient. While maintaining the image quality as much as possible.But it is worth noting that Limiting angle CT reconstruction reduces image quality with the production of Streaking artifact, and this is our new research question: How can Streaking artifact be reduced? What algorithm do we need to reduce distortions and maintain image quality to provide an accurate diagnosis?

References

1. Almasri, H. and Inayyem, W. (2021) 'Evaluation of radiation doses for patients undergoing abdominopelvic computed tomography examination in Palestine', *Japanese Journal of Health Physics*, 56(2), pp. 75–79. doi: 10.5453/JHPS.56.75.

2. Alsleem, H. and Davidson, R. (2013) 'Factors affecting contrast-detail performance in computed tomography: A review', *Journal of Medical Imaging and Radiation Sciences*, 44(2), pp. 62–70. doi: 10.1016/j.jmir.2012.12.001.

3. Anirudh, R. *et al.* (2018) 'Lose the Views: Limited Angle CT Reconstruction via Implicit Sinogram Completion', *Proceedings of the IEEE Computer Society Conference on Computer Vision and Pattern Recognition*, pp. 6343–6352. doi: 10.1109/CVPR.2018.00664.

4. Barutcu, S. *et al.* (2021) 'Limited-angle computed tomography with deep image and physics priors', *Scientific Reports*, 11(1), pp. 1–12. doi: 10.1038/s41598-021-97226-2.

5. Beister, M., Kolditz, D. and Kalender, W. A. (2012) 'Iterative reconstruction methods in X-ray CT', *Physica Medica*, 28(2), pp. 94–108. doi: 10.1016/j.ejmp.2012.01.003.

6. Calzado, A., Rodríguez, R. and Muñoz, A. (2000) 'Quality criteria implementation for brain and lumbar spine CT examinations', *British Journal of Radiology*, 73(868), pp. 384–395. doi: 10.1259/bjr.73.868.10844864.

7. Crawford, F. R. and Kina, K. F. (1990) 'Measurement of the presampling modulation transfer function of film digitizers using a curve fitting technique', *Medical Physics*, 17(6), pp. 967–982. doi: 10.1118/1.596464.

8. 'DMIP22-K3006-Reconstruction-From-Limited-Angle-Projections-Based-on-Transformation-1' (no date).

9. Eliason, N. E. (2022) *A Textbook, American Speech*. doi: 10.2307/486972.

10. Funama, Y. *et al.* (2005) 'Radiation dose reduction without degradation of low-contrast detectability at abdominal multisection CT with a low-tube voltage technique: Phantom study', *Radiology*, 237(3), pp. 905–910. doi: 10.1148/radiol.2373041643.

11. Gong, C. and Zeng, L. (2020) 'Self-Guided Limited-Angle Computed Tomography

Reconstruction Based on Anisotropic Relative Total Variation', *IEEE Access*, 8, pp. 70465–70476. doi: 10.1109/ACCESS.2020.2985107.

12. Guo, J. *et al.* (2016) 'Iterative Image Reconstruction for Limited-Angle CT Using Optimized Initial Image', *Computational and Mathematical Methods in Medicine*, 2016. doi: 10.1155/2016/5836410.

13. Hata, A. *et al.* (2018) 'Effect of Matrix Size on the Image Quality of Ultra-high-resolution CT of the Lung: Comparison of 512×512, 1024×1024, and 2048×2048', *Academic Radiology*, 25(7), pp. 869–876. doi: 10.1016/j.acra.2017.11.017.

14. Hobbs, J. B. *et al.* (2018) 'Physician Knowledge of Radiation Exposure and Risk in Medical Imaging', *Journal of the American College of Radiology*, 15(1), pp. 34–43. doi: 10.1016/j.jacr.2017.08.034.

15. Hu, Z. *et al.* (2017) 'An improved statistical iterative algorithm for sparse-view and limited-angle CT image reconstruction', *Scientific Reports*, 7(1), pp. 1–9. doi: 10.1038/s41598-017-11222-z.

16. Jaffray, D. A. and Siewerdsen, J. H. (2000) 'Cone-beam computed tomography with a flat-panel imager: Initial performance characterization', *Medical Physics*, 27(6), pp. 1311–1323. doi: 10.1118/1.599009.

17. Kak, A.C., S. M. (no date) 'Principles of Tombgraphic Imaging', *Book*.

18. Kalender, W. A. *et al.* (1990) 'Spiral volumetric CT with single-breath-hold technique, continuous transport, and continuous scanner rotation', *Radiology*, 176(1), pp. 181–183. doi: 10.1148/radiology.176.1.2353088.

19. Kalra, M. K. *et al.* (2004) 'Strategies for CT Radiation Dose Optimization', *Radiology*, 230(3), pp. 619–628. doi: 10.1148/radiol.2303021726.

20. King, A. B., McCarter, L. and Davis, J. S. (1982) 'Dextrostix reactivity variation.', *Diabetes care*, 5(5), p. 555. doi: 10.2337/diacare.5.5.555a.

21. Kohl, G. (2005) 'The evolution and state-of-the-art principles of multislice computed tomography', *Proceedings of the American Thoracic Society*, 2(6), pp. 470–476. doi: 10.1513/pats.200508-086DS.

22. Lee, T. Y. and Chhem, R. K. (2010) 'Impact of new technologies on dose reduction

in CT', *European Journal of Radiology*, 76(1), pp. 28–35. doi: 10.1016/j.ejrad.2010.06.036.

23. McCollough, C. H. *et al.* (2009) 'Strategies for Reducing Radiation Dose in CT', *Radiologic Clinics of North America*, 47(1), pp. 27–40. doi: 10.1016/j.rcl.2008.10.006.

24. Nakayama, Y. *et al.* (2005) 'Abdominal CT with low tube voltage: Preliminary observations about radiation dose, contrast enhancement, image quality, and noise', *Radiology*, 237(3), pp. 945–951. doi: 10.1148/radiol.2373041655.

25. National Research Council (2006) 'BEIR VII: health risks from exposure to low levels of ionizing radiation: report in brief', *National Academies*, (93), pp. 93–96. Available at: https://nap.nationalacademies.org/resource/11340/beir_vii_final.pdf.

26. Qi, H. *et al.* (2016) 'Iterative image reconstruction using modified non-local means filtering for limited-angle computed tomography', *Physica Medica*, 32(9), pp. 1041–1051. doi: 10.1016/j.ejmp.2016.07.310.

27. Romans, L. E. (2011) 'Computed Tomography for Technologists A Comprehensive Text by Lois E. Romans 2010'.

28. Seibert, J. A. (2014) 'Iterative reconstruction: how it works, how to apply it', *Pediatric Radiology*, 44(3), pp. 431–439. doi: 10.1007/s00247-014-3102-1.

29. Tepper, S. J. (2008) 'Computed tomography - An increasing source of radiation exposure: Commentary', *Headache*, 48(4), p. 657. doi: 10.1111/j.1526-4610.2008.01071.x.

30. Toth, T. L. *et al.* (2005) 'Image quality and dose optimization using novel x-ray source filters tailored to patient size', *Medical Imaging 2005: Physics of Medical Imaging*, 5745, p. 283. doi: 10.1117/12.595465.

31. Willemink, M. J. and Noël, P. B. (2019) 'The evolution of image reconstruction for CT—from filtered back projection to artificial intelligence', *European Radiology*, 29(5), pp. 2185–2195. doi: 10.1007/s00330-018-5810-7.

32. Wilting, J. E. *et al.* (2001) 'A rational approach to dose reduction in CT: Individualized scan protocols', *European Radiology*, 11(12), pp. 2627–2632. doi: 10.1007/s003300101039.

33. Xu, M. *et al.* (2021) 'Limited-Angle X-Ray CT Reconstruction Using Image Gradient ℓ0-Norm with Dictionary Learning', *IEEE Transactions on Radiation and Plasma Medical Sciences*, 5(1), pp. 78–87. doi: 10.1109/TRPMS.2020.2991887.

34. Yu, L. *et al.* (2009) 'Radiation dose reduction in computed tomography: techniques and future perspective', *Imaging in Medicine*, 1(1), pp. 65–84. doi: 10.2217/iim.09.5.

35. Yu, W. and Zeng, L. (2015) 'ℓ 0 Gradient Minimization Based Image Reconstruction for Limited-Angle Computed Tomography', *PLoS ONE*, 10(7), pp. 1–15. doi: 10.1371/journal.pone.0130793.

36. Zeng, G. L. (2010) *Medical Image Reconstruction*, *Medical Image Reconstruction*. doi: 10.1007/978-3-642-05368-9.

نهج متقدم لإعادة بناء الصور المقطعية من الإسقاطات ذات الزاوية المحدودة، مما يقلل من الإشعاع الجرعة وحمل الأنبوب

دعاء حسني علي بني عودة

اشراف: د. محمد حجوج

الملخص:

إنَّ التطوراتِ الكبيرةَ لجهازِ التصويرِ المقطعيّ المحوسبِ والاقبالِ على استخدامِهِ كجهازٍ تشخيصيٍّ دقيق , أدى الى زيادةِ الطلبِ المستمرِ عليهِ وبالتّالي زيادةِ مخاطرِ الجهازِ على المرضى من حيث زيادة الاشعاع المؤيّن على المرضى ، الأمرُ الذي دفعَ كثيراً من الباحثينَ إلى إيجادِ طرقٍ تساعدُ في تقليلِ جرعةِ الاشعةِ المؤينةِ الموجهةِ للمريضِ معَ المحافظةِ على جودةِ الصورةِ حسبَ مبدأ . (ALARA) لذلكَ تعتبرُ هذهِ الدراسةُ احدى المحاولاتِ في تقديمِ منهجٍ جديدٍ لتقليلِ جرعةِ الاشعةِ المؤينةِ الموجهةِ للمريضِ , حيث يهدف الباحثون في هذهِ الدراسةِ إلى التحققِ من إمكانيةِ تكوينِ صورةٍ مقطعيةٍ محوسبةٍ للدماغِ من عددٍ لا يتجاوزُ الخَمسة مئةِ اسقاطٍ شعاعيّ بزاويةٍ اقلُّ من مئةٍ وثمانينَ درجةٍ(180درجة) فيما يسمى (Limited angle CT reconstruction) معَ الحفاظِ على جودةِ الصورة، وتقليلِ جرعةِ الاشعاعِ المستخدمة . وأيضاً تمَّ التحققُّ من إذا كانت الصورةُ الناتجةُ تتوافقُ معَ معاييرِ الجودةِ لصورِ الدماغَ المقطعية . امتدّت هذهِ الدِّراسةُ مِنْ شهرِ يناير 2023 إلى شهرِ سبتمبر 2023.

تُعَدُّ عمليةُ إعادةِ بناءِ صورِ الأشعةِ المقطعيةِ من إسقاطاتٍ ذاتَ زاويةٍ محدودةٍ أمْراً بالغِ الأهمية ، وتتطلبُ التزامًا صارمًا بمبدأ (ALARA) تم تصميمُ هذا المبدأِ لتقليلِ التعرضِ للإشعاعِ معَ الحفاظِ على جودةِ الصورة. استخدمتْ دراستُنا برنامج(MATLAB 2021) ّلإعادةِ بناءِ صورِ التصويرِ المقطعيَ المحوسب للدماغِ باستخدامِ مرشحِ الإسقاطِ الخلفيّ (FBP) وخوارزمياتِ إعادةِ البناءِ التكراريّ الجبريّ (IR) لإعادةِ بناءِ صورِ الأشعةِ المقطعية للدماغِ من خمسَة مئةِ اسقاطٍ(500) شعاعيّ بحجمِ مصفوفةِ 100 × 100 ، و200 × 200. بالإضافةِ إلى بحثِ تأثيرِ زاويةِ إعادةِ البناءُ على جودةِ الصورة، تمَّ استخدامُ زاويتين للإسقاطِ الشعاعيّ (90 و45 درجة). تمَّ تقييمُ الصورِ وفقًا لمعاييرِ جودةِ الصورة من قِبَلِ 10 فنيينَ خُبراء في التصويرِ المقطعيّ المحوسب واثنانِ من أخصائي الأشعةِ وتمَّ إجراءُ تقييماتٍ محددة. بعدَ ذلك، تمَّ إجراءُ تحليلٍ إحصائيٍّ وصفيٍّ بسيط، بما في ذلكَ حسابَ النسبِ المئوية لتقييماتِ فنيّي التصويرِ الطبيِ وأخصائي الأشعةِ الخبراء والقيمِ الاحتمالية.

من خلال الجمع بينَ نتائج برنامج (MATLAP 2021) ورؤى أخصائي الأشعة ، يمكنُنا إنتاجَ صورٍ عاليةِ الجودةِ تقللُّ منْ جرعةِ الإشعاعِ وحملِ الأنبوب. تكشفُ النتائجُ التي توصلّنا إليها أنَّ الطريقةَ الجبرية تتفوقُ على الإسقاطِ الخلفيّ للمرشحِ في الحفاظِ على جودةِ الصورة عندَ استخدامِ الإسقاطاتِ ذاتَ الزاويةِ المحدودة. بالإضافةِ إلى إنتائج الاختبارِ

الاحصائيّ(t-test) (P<.001)الذي يؤكدُّ وجودَ فروقٍ إحصائية بين الخوارزميتين. حيثُ شكلتْ خوارزميةُ إعادةِ البناء التكراريةِ الجبرية (IR) نسبةَ 41% منْ مجموعِ النِّسبِ المئوية لتقييمِ اخصّائي الأشعة ، أو ما يعادلُ تقديرَ متوسط حسبَ المعاييرِ المقدمة لأخصائي الأشعة في الاستبيانِ الموَزَّع ، تتوافقُ خوارزميةُ إعادةِ البناءِ الجبرية (IR) معَ متطلباتِ الجودة بشكلٍ أفضل. وعلى العكسِ منْ ذلك، يُظهرْ FBP نسبةَ أقل مِن 25%، ممّا يدلُ على تقديرٍ ضعيف حسبَ التقييماتِ المعتمدة في الاستبيان.

اعتماداًعلى النسبِ المئوية يُمكنُنا أن نُؤكدَ أنَّ حجمَ المصفوفةِ 200×200 يتفوقُ على حجمِ المصفوفةِ 100×100، ح يثُ شكلتْ نسبة 36.25% منْمعدلِ نسبِ تقييماتِ اخصّائي الأشعةِ ، وهوَ ما يُعادلُ مقياسَ متوسط،الذي يؤكدُ تفوقَ ح جمَ المصفوفة 200×200 على الاخرى, بالإضافةِ إلىذلك فإن زاويةَ إعادةِ البناءِ البالغة 90 تؤَفرُ جودةً أفضَلْ وكانَتْ نِسبتها41.75% أي ما يعادِلُ مقياسَ متوسط. لذا فإن خوارزميةَ اعادةِ البناءِالجبرية عندَ 90 درجة معَ 500 إسقاطٍ ع لى حجمِ مصفوفة 200×200 توفرُ صورًا تتوافقُ معَ معاييرِ الجودةِ للتصويرِ المقطعيّ للدماغ. بينمايَفشلُ FBP في تقديمِ أي رؤى مفيدة عند العملِ بزوايا 45 و90 درجة.

APPENDICES

APPENDIX A

Al Quds University

Faculty of Health Professions

Medical Imaging Department

Jerusalem –Abu Dies

جامعة القدس
كلية المهن الصحية
دائرة التصوير الطبي
القدس- أبوديس

تقوم الباحثة دعاء بني عودة من برنامج الدراسات العليا - دائرة التصوير الطبي \ جامعة القدس بهذه لدراسة للبحث عن:

(تطوير انتاج صور طبيقة من زوايا محدوده نحو تقليل الجرعات الاشعاعية وتقليل احمال تيوب الاشعة). بعنوان:

CT image reconstruction from limited angel projections.

هذا الاستبيان موجه للخبراء في مجال التصوير الطبقي وقراءة الصور الطبقية

نرجو من حضرتكم التكرم بتخصيص دقائق من وقتكم لتعبئة هذا الاستبيان بناءة على نقاط التقييم الاربعة ادناه

ولكم كل الشكر.

Please answer all questions based on the below four-point criteria using your experience with CT scans.

Many thanks.

I. Demographic information:

Age	22-30	31-40	41-50	51-60	>60	العمر
Gender	M					الجنس
Workplace	Public Health Center or Hospital	NGO Health Center or Hospital	Private Health Center or Hospital	Private Clinic	خدمات طبية عسكرية	مكان العمل

Experience	≤ 5 years	6-10	11-20	21-30	> 30	سنوات الخبرة
Specialty	Consultant Radiologist	Radiology resident Physician		CT Technician		مسمى التخصص

Images evaluation Criteria:

Visual grading characteristics:

1. Visually sharp reproduction of the border between white and grey matter.
2. Visually sharp reproduction of the basal ganglia.
3. Visually sharp reproduction of the ventricular system.
4. Visually sharp reproduction of the cerebrospinal fluid space over the brain.

(1: weak, 2: moderate, 3: accepted, 4: perfect)

Reconstructed image	Reconstruction algorithm	Evaluation	Reconstruction algorithm	Evaluation	Reconstruction algorithm	Evaluation	Reconstruction algorithm	Evaluation
Case 1	Figure 1: a)	1	Figure 2: a)	1	Figure 3: a)	1	Figure 4: a)	3
	Figure 1: b)	1	Figure 2: b)	1	Figure 3: b)	1	Figure 4: b)	1

Case 2	Figure 1: a)	1	Figure 2: a)	1	Figure 3: a)	1	Figure 4: a)	3
	Figure 1: b)	1	Figure 2: b)	1	Figure 3: b)	1	Figure 4: b)	1
Case 3	Figure 1: a)	1	Figure 2: a)	2	Figure 3: a)	1	Figure 4: a)	2
	Figure 1: b)	1	Figure 2: b)	1	Figure 3: b)	1	Figure 4: b)	1